Uplift Resistance of an Under-reamed Pile Foundation

by

Fiona Hughes (Q)

Fourth-year undergraduate project

in Group D, 2014/2015

"I hereby declare that, except where specifically indicated, the work submitted herein is my own original work"

Signed: **Date:**

Technical Abstract

Under-reamed pile foundations are a type of pile foundation with an enlarged base cross section designed to provide uplift resistance. For this reason, they are currently used as foundations for low self-weight structures that are subject to high lateral loads and for sites with expansive soils. Layered soils are frequently encountered by practising engineers, hence the behaviour of under-reamed piles in layered soil must be understood. However, very little experimental research has been conducted in this area. The main objective of this project was to address this lack of information.

Two types of small scale model tests were conducted at 1-g to investigate the uplift behaviour of smooth under-reamed pile foundations in dry two-layered sand. The first set consisted of standard pullout tests to determine the load-displacement response of the under-reamed piles. The second consisted of half space model tests and subsequent Particle Image Velocimetry (PIV) analysis to characterise the failure mechanism geometry of a smooth, 45° under-reamed pile in dry, two-layered sand. All layered tests conducted had a dense lower layer and a loose upper layer of sand with the ratio of the lower layer thickness to the total embedment depth being varied, whilst keeping the total embedment depth constant. The experimental results were compared to simple upper and lower bound theoretical solutions used to calculate the capacity of foundations and to published literature on plate anchors and under-reamed pile foundations in non-cohesive soil.

From the pullout tests conducted in this project, the load-displacement behaviour of under-reamed piles in two-layered sand was found to display a peak capacity followed by a post-peak reduction in capacity. The initial stiffness response of the piles in two-layered sand was observed to be the same as for homogeneous dense sand. However, the presence of a loose upper layer was found to both reduce the stiffness response as peak capacity is approached and also to significantly reduce the peak uplift capacity of the piles. The peak uplift capacities of the model plate anchor and of the 30° and 45° under-reamed pile foundations tested were found to be very similar for a given two-layered sand configuration. An approximately linear relationship was observed between the peak uplift capacity and the ratio of dense lower layer thickness to the total embedment depth.

The PIV analysis of the half space model tests conducted in this project was used to characterise the failure mechanism geometry for a smooth, 45° under-reamed pile in two-layered sand. At small strains, resistance was observed to only be mobilised in the lower dense layer. The small strain failure mechanisms were very similar for all the two-layered sand configurations tested, hence explaining the same initial stiffness response for the under-reamed piles in the different layering configurations. In contrast, at peak capacity, the layering configuration was found to have a significant effect on the failure mechanism mobilised. At peak capacity, the dense lower layer was seen to mobilise large displacements. If only a shallow layer of loose sand was present, all the strains were mobilised in the loose layer and the displacements reached the ground surface. However, if a sufficiently thick layer of loose sand were present, the displacements were prevented from reaching the ground surface by local compaction of the loose sand layer. The soil displacement vectors immediately above the under-ream were observed to be approximately vertical and not at an angle to the under-ream. At peak capacity smooth, 45° under-reamed piles therefore behave like plate anchors in two-layered sand, hence explaining the similar peak uplift capacities obtained for the plate anchor and for the two under-reamed piles tested in the pullout tests.

Post-peak, all the strains were observed to be mobilised in the loose upper layer and the displacements reached the ground surface for all two-layered configurations tested. The mean inclination of the soil displacement vectors immediately above the under-ream across all three tests was found to be approximately equal to the interface friction angle between the under-ream and the sand. As expected, a proposed lower bound solution, which assumed that the principal stress direction is rotated by an angle equal to that of the interface friction angle, underestimates the experimental post-peak uplift capacity of the model under-reamed piles. In contrast, a solution based on the upper bound theorem of plasticity was found to be inappropriate for estimating the response of the model under-reamed pile foundations in dry two-layered sand due to the incorrect assumption that normality is observed.

The implications of this research on the practical design of under-reamed piles are that if a pile embedded in a dense sand layer will only be subject to small strains, its performance will not be affected by the presence of a loose upper layer, provided there is a sufficient layer of dense sand above the under-ream. However, if the design relies upon the peak capacity or post-peak capacity, the performance of the pile will be significantly affected by the presence of a loose upper layer.

Table of Contents

Nomenclature

D	Pile base diameter [m]
D_{50}	Particle size at which 50% of the particles are finer by weight [m]
e	Voids ratio [-]
H	Embedment depth of the pile measured from the soil surface to the point of widest diameter [m]
h_1	Upper layer thickness [m]
h_2	Lower layer thickness [m]
Q	Uplift capacity [N]
N	Dimensionless uplift capacity [-]
y	Pile head displacement [m]
γ	Soil unit weight [kN/m^3]
δ	Pile-soil interface friction angle [°]
θ	Pile under-ream angle measured from the horizontal [°]
σ	Stress [Pa]
τ	Shear stress [Pa]
ϕ	Internal soil friction angle [°]

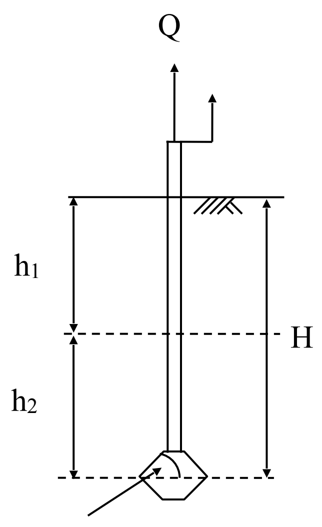

Figure (i): Experimental setup.

1. Introduction

1.1 Under-reamed pile foundations

Under-reamed pile foundations are a type of pile foundation with an enlarged base cross section designed to increase the compressive capacity of a pile or to provide uplift resistance. They are also known as mushroom foundations (Balla, 1961) and belled piles or piers (Dickin & Leung, 1990; Dickin & Leung, 1992). Under-reamed piles are currently used in several different situations to provide uplift capacity, including:

- foundations for low self-weight structures that are subject to high lateral loads. This includes lightweight steel frame buildings and structures, such as electricity pylons, and some offshore structures.
- for sites with expansive soils where the swelling of the soil due to an increase in water content causes an uplift force on the structure. This includes sites with soils containing large quantities of minerals from the montmorillonite group, such as Black Cotton Soil, which is commonly found in India (Nagelschmidt et al., 1940).

Under-reamed piles are more economical in cost and material usage than large gravity based foundations that have historically been used (Dickin & Leung, 1990).

Under-reamed piles can be cut by rotating a belling bucket within a previously drilled straight sided shaft (figure 1) or can be placed in a previously excavated pit, with the earth then filled in and compacted around the pile (Balla, 1961).

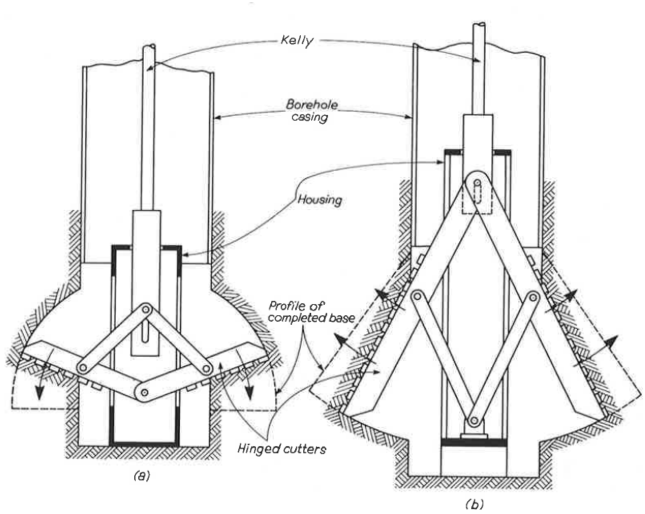

Figure 1: Under-reaming tools: (a) bottom hinge, (b) top hinge (Tomlinson, 2001).

Under-reamed piles are predominantly used in India and South East Asia (Harris & Madabhushi, 2015), and guidelines for their design and construction are provided in the Indian Standard IS 2911-3 (Bureau of Indian Standards, 1980). Here the equation given to calculate the ultimate uplift capacity of under-reamed pile foundations in sandy soil is the same as that used to calculate the bearing capacity, but with the term related to the bearing on the tip removed. No consideration is made to the difference in failure mechanism between bearing and uplift.

1.2 Motivation for work

Foundations must be designed to satisfy both safety and serviceability requirements. To be able to do this, and also to ensure that foundations remain economical, the load displacement behaviour and the failure mechanism geometry must be understood. The theory behind the uplift resistance of plate anchors in homogeneous noncohesive soil is relatively well understood and progress has been made to characterise the behaviour of plate anchors in two-layered noncohesive soil. However, there is lack of academic research in the area of under-reamed pile foundations, particularly in layered sand. The aim of this project was to begin to characterise the behaviour of under-reamed pile foundations in two-layered sand.

1.3 Problem definition

This research follows on directly from the work conducted by Harris (2014). Small scale, displacement controlled tests, conducted at 1-g, were used to examine the uplift capacity, load displacement response and failure mechanism geometry of smooth under-reamed pile foundations in dry, two-layered sand. This research used model aluminium piles in two-layered sand, with a lower dense layer overlain by an upper loose layer. The ratio of the lower layer thickness to the total embedment depth (h_2/H) was varied whilst keeping the total embedment depth ($H = h_1+h_2$) constant. This research forms a comparative study but should not be used to predict the load response or settlement of fully sized under-reamed piles, since small scale model tests conducted at 1-g have much smaller soil confining stress levels than are usually experienced in the field.

1.4 Project objectives

The intentions of this project were to:

- compare the uplift capacity and load-displacement characteristics of smooth under-reamed pile foundations using standard pullout tests, with a focus on comparisons between homogeneous sand and two-layered sand with different layering configurations.

- characterise the uplift failure mechanism of smooth under-reamed pile foundations in two-layered sand using Particle Image Velocimetry (PIV) analysis, investigating the effect the lower layer thickness has on the mechanism geometry.
- compare the experimental results to simple upper and lower bound theoretical solutions used to calculate the capacity of foundations.
- compare the experimental results to published literature on plate anchors and under-reamed pile foundations.

2. Review of Literature

Murray & Geddes (1987) proposed the notation for dimensionless uplift capacity, $N = \frac{Q}{\gamma' AH}$.

Where A is the maximum cross sectional area of the enlarged base. This notation has been consistently used in preceding literature, and will be used throughout this report.

For the purpose of this literature review, the relative densities for loose, medium-dense and dense sand are < 40%, 40-65% and > 65% respectively.

2.1 Uplift capacity of plate anchors in homogeneous sand

1. Experimental studies

Numerous studies have been conducted to investigate the effect of anchor diameter, embedment depth, and sand density on the uplift capacity of plate anchors in homogeneous sand. The majority of this research has been experimental and has involved small scale testing conducted at 1-g. The uplift capacity of plate anchors in homogeneous sand has been observed to increase with embedment depth (Meyerhof & Adams, 1968; Rowe & Davis, 1982; Dickin, 1988; Ilamparuthi et al., 2002). The uplift capacity has also been found to increase with increasing plate diameter (Hopkins, 2013), increasing sand friction angle (Meyerhof & Adams, 1968) and with increasing sand density (Murray & Geddes, 1987; Dickin, 1988; Ilamparuthi et al., 2002; Hopkins, 2013; Harris & Madabhushi, 2015).

Ilamparuthi et al. (2002) found the load-displacement behaviour of circular plate anchors to be independent of the density of the sand, but to be dependent on whether the anchor was shallow (the failure mechanism extended to the ground surface) or deep (the failure mechanism did not extend to the ground surface). They observed that shallow plate anchors exhibited three-phase behaviour similar to that observed for dense sand subject to direct shear, and that deep plate anchors exhibited two phase behaviour similar to that observed for loose sand subject to direct shear. In addition, Ilamparuthi et al. (2002) used six different methods to identify the critical embedment ratio (H/D), where the pile behaviour transitioned from shallow to deep, and found it to be linearly dependent upon the friction angle. Meyerhof

& Adams (1968) had also observed a critical embedment depth, which they found to be dependent upon the friction angle but had not observed a linear relationship between the two.

In comparison, very few centrifuge testing programmes have been undertaken to determine the uplift capacity of plate anchors in cohesionless soil. Dickin (1988) observed a significant disparity in the capacity of model anchors tested under simple gravity and centrifuge loading, with the former yielding much higher capacities. He concluded that using the results of small scale 1-g tests to predict the capacity of full size plate anchors will produce overoptimistic predictions.

Throughout the experimental research conducted there is agreement that the uplift capacity of plate anchors is a combination of the frictional resistance along the failure surface and the weight of the soil within it. However, there is no agreed theory for defining the shape of the failure surface due to the difficulty in characterising the failure mechanism geometry (Meyerhof & Adams, 1968; Murray & Geddes, 1987; Ilamparuthi et al., 2002). Ilamparuthi et al. (2002) conducted an extensive literature review on the proposed failure mechanism geometries and highlighted three main geometries for shallow anchors which had been proposed in literature prior to 2002. These are the vertical slip surface model (VSSM), the soil cone model and the circular arc model (figure 2). The failure mechanism geometry for deep anchors has not been researched in depth, but both Ilamparuthi et al. (2002) and Harris & Madabhushi (2015) observed “balloon” shaped mechanisms that were symmetrical about the anchor axis.

Post failure fluctuations in load have been observed in both loose sand (Dickin, 1988; Ilamparuthi et al., 2002; Hopkins, 2013) and dense sand (Murray & Geddes, 1978; Rowe & Davis, 1982; Dickin, 1988; Ilamparuthi et al., 2002; Hopkins, 2013) and have been attributed

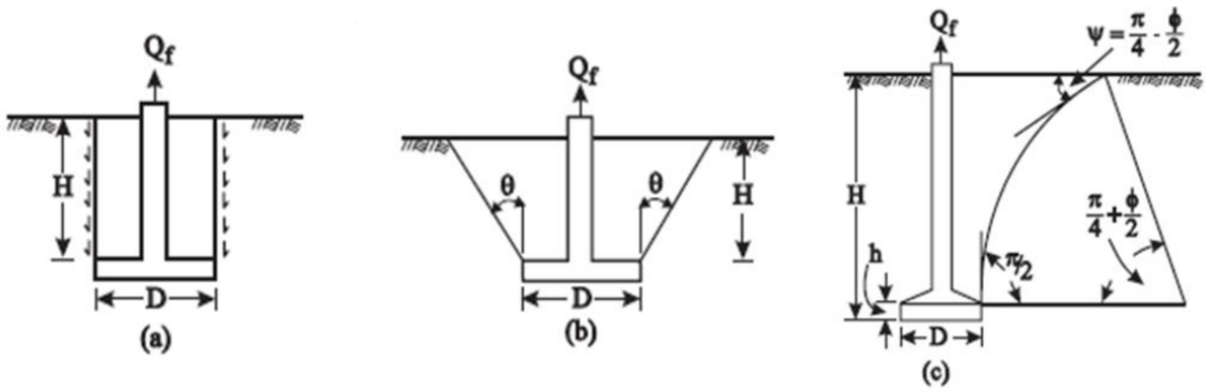

Figure 2: Assumed failure surfaces for shallow anchors: (a) vertical slip surface model, (b) soil cone model, and (c) circular arc model (Ilamparuthi et al., 2002).

to the collapse and flow of sand from above the anchor towards the gap created below it (Ilamparuthi et al., 2002).

2. Theoretical models

Theoretical models have been used to predict the uplift capacity of plate anchors in homogeneous sand. These models can be broadly classified into two categories: limit equilibrium (White et al., 2008) and plasticity solutions (Murray & Geddes, 1987; White et al., 2008). Through comparison with an extensive database of 115 model tests on pipes and strip anchors, White et al. (2008) found the limit equilibrium solution captures the observed failure mechanism well and yields accurate predictions of the uplift capacity. However, solutions based on the limit theorems of plasticity were found to be inappropriate (White et al. 2008) since they require normality to be observed. Normality is not observed when modelling the uplift capacity of plate anchors in dry sand (White et al. 2008). Therefore, solutions based on the limit theorems of plasticity overestimate the volume of sand within the failure mechanism and ignore the frictional resistance along the failure surface because there is no internal energy dissipation when normality is observed (Cheuk et al., 2008). These solutions have been found to be to be unconservative for plate anchors in homogeneous sand (Murray & Geddes, 1987; White et al., 2008).

More rigorous numerical studies have been performed to investigate the performance of plate anchors in homogeneous sand (Rowe & Davis, 1982; Merifield & Sloan, 2006). Rowe & Davis (1982) used an elastic finite element analysis, whilst Merifield & Sloan (2006) used both the upper and lower bound theorems of limit analysis and the displacement finite element technique. Both found the dimensionless ultimate uplift capacity of a plate anchor to increase linearly with soil friction angle and found the interface roughness of the anchor to have negligible effect on the uplift capacity. Rowe & Davis (1982) also observed a linear increase in the uplift capacity with embedment ratio (H/D), for a given friction angle, as predicted by Meyerhof & Adams (1968), and found the initial stress state had little effect on the ultimate capacity. They also adopted both associated and non-associated flow rules, and found that soil dilatancy appreciably increased the ultimate capacity of anchors at moderate depth ($H/D > 3$) in medium-dense to dense sand ($\phi > 30°$). Merifield & Sloan (2006) did not observe any plastic shearing or flow below the anchor in any of their numerical studies, and did not observe a critical embedment ratio, the latter being in contrast to the experimental results of Meyerhof & Adams (1968) and Ilamparuthi et al. (2002). These two numerical studies (Rowe & Davis, 1982; Merifield & Sloan, 2006) were found to yield results that were in reasonable agreement to experimental data (Rowe & Davis, 1982; Murray & Geddes, 1987), but tended to slightly overestimate the uplift capacities of the plate anchors.

2.2 Uplift capacity of under-reamed pile foundations in homogeneous sand

In comparison to plate anchors, very few studies have been conducted to investigate the uplift capacity of under-reamed pile foundations in homogeneous sand.

Balla (1961) was one of the first to investigate the uplift resistance of piles with enlarged bases. He conducted small scale model tests at 1-g and used his semi-partial model test results, in conjunction with Kotter's equation, to derive an equation for the ultimate capacity of under-reamed pile foundations. The derived formula was found to predict the ultimate capacity of previous full scale tests made in situ with "reasonably close" agreement. However, only five comparisons were made. The trends observed for under-reamed piles were in agreement with those for plate anchors in section 2.1.

Dickin & Leung conducted two series of model tests on under-reamed pile foundations in sand (Dickin & Leung, 1990; Dickin & Leung, 1992). The first consisted of an extensive centrifuge model test programme to examine the influence of under-ream diameter, embedment depth, and soil unit weight on the uplift behaviour of under-reamed pile foundations in homogeneous sand (Dickin & Leung, 1990). The uplift capacity of under-reamed pile foundations was found to be strongly dependent on embedment ratio (H/D) and sand density, and increased with increases in both. In dense and medium-dense sand, a well defined ultimate capacity was observed, with a significant post-peak reduction in capacity, whereas in loose sand no such reduction was observed. The load displacement behaviour in loose sand exhibited a distinct "kink", which was thought to be due to a transition in failure mechanism from around the base to a more generalised movement in sand mass, but was not investigated further. The normalised uplift capacity of under-reamed piles obtained in these centrifuge model tests were comparable to previous centrifuge model test results for plate anchors (Dickin, 1988). However, design equations for plate anchors derived from small scale model tests conducted at 1-g were found to considerably over-predict the uplift capacity of the under-reamed piles in both homogeneous dense and homogeneous loose sand.

The second investigation conducted by Dickin & Leung into the uplift behaviour of under-reamed piles in homogeneous sand involved centrifuge tests to investigate the effect of the under-ream angle on the uplift capacity (Dickin & Leung, 1992). The uplift capacity was found to significantly reduce with increased under-ream angle in both dense and loose sand, with the reduction being most marked for under-ream angles greater than 62°. They also conducted semi-cylindrical model tests at 1-g to investigate the failure mechanisms for under-reamed pile foundations. In loose sand, failure within the soil mass was not observed with relative movement being restricted to the under-ream-sand interface. In dense sand the partial development of a rupture plane in the sand mass was observed, but was markedly less than that observed for plate anchors in previous studies (Meyerhof & Adams, 1968; Rowe & Davis, 1982; Dickin, 1988). Dickin & Leung (1992) proposed simple equations and graphs to compare the uplift resistance of under-reamed pile foundations to plate anchors. For an under-ream angle of 45° and an under-ream diameter twice that of the shaft, the relationship between embedment ratio (H/D) and the ratio of normalised uplift resistance for under-reamed pile foundations to plate anchors was found to be essentially independent of sand unit weight and constant for an embedment ratio greater than three.

Hopkins (2013) and Harris & Madabhushi (2015) each conducted a series of small scale model tests at 1-g to compare the behaviour of plate anchors and piles with under-reams of different angles. Both found that the load-displacement behaviour of plate anchors and under-reamed piles closely followed the expected behaviour of sand subjected to simple shear, with loose sand exhibiting contractile behaviour with no peak strength above the critical state and dense sand showing initially dilatory behaviour, followed by post-peak softening towards a critical state. This observation is consistent with the results obtained by Dickin & Leung (1992) but is in disagreement with the results of Ilamparuthi et al. (2002) for plate anchors. Both Hopkins (2013) and Harris & Madabhushi (2015) found the uplift capacity of under-reamed piles in loose sand to decrease as the under-reaming angle increases, and Harris & Madabhushi (2015) found that in dense sand an optimum uplift capacity was observed with an under-ream angle of approximately 45° - $\phi/2$. Harris & Madabhushi (2015) also found that the experimental uplift resistance of under-reamed pile foundations was less than that predicted by Meyerhof & Adams (1968) for a flat plate, when both a conical failure surface and a cylindrical (VSSM) failure mechanism is assumed.

Harris & Madabhushi (2015) used half space model tests and PIV analysis to observe the failure mechanism of a plate anchor and a 45° under-reamed pile in homogeneous sand and found that the uplift failure mechanism changed with both the sand density and the under-ream angle. The under-ream angle was found to have a noticeable effect on the failure mechanism geometry close to the pile base, but reduced as the distance from the base increased. In loose sand, a 45° under-reamed pile behaved as a deep pile with a "balloon" shaped mechanism, whereas in dense sand, a roughly conical failure mechanism was observed, this extending to the soil surface.

2.3 Uplift capacity of plate anchors in two-layered sand

In contrast to homogeneous sand, very little research has been conducted to investigate the uplift capacity of plate anchors in two-layered non-cohesive soil, despite it being a problem which is frequently encountered by practising engineers (Bouazza & Finlay, 1990).

The first work to determine the ultimate uplift capacity of a plate anchor in two-layered sand was conducted by Bouazza & Finlay (1990). Model tests at 1-g were conducted for shallow plate anchors with a loose or medium-dense sand layer overlying a dense lower layer. They defined the upper thickness ratio λ to be the ratio of upper layer thickness to anchor diameter ($\lambda = h_1/D$). For $\lambda = 1$ it was found that the ultimate uplift capacity was independent of the state of the upper layer (loose or medium), suggesting that, for this particular case, the dense layer is providing most of the strength. For $1 < \lambda \leq 4$ the load displacement relationship was found to be dependent of the type of upper layer. For a given embedment ratio (H/D), the uplift capacity increased with increasing thickness of the dense lower layer, and was higher for a medium-dense upper layer than a loose upper layer.

Kumar (2003) used the upper bound theory of limit analysis to find the vertical uplift capacity of shallow strip and circular plate anchors in two-layered sand. He assumed that the velocity discontinuities were linear and that the rupture surfaces reached the ground surface. The soil was also assumed to follow an associated flow rule. The critical collapse mechanism was found to involve the entire soil wedge lying above the plate anchor to move as a single rigid block, with the same velocity as the anchor itself, which is similar to that obtained by Murray & Geddes (1987) for plate anchors in homogeneous sand. The theoretical uplift capacity obtained using this method was found to be a little higher than, but in reasonable agreement with, the experimental results of Bouazza & Finlay (1990) for shallow plate anchors.

Sakai & Tanaka (2007) used model tests conducted at 1-g and elastoplastic finite-element analysis, which considered progressive failure with shear band effect, to investigate the uplift capacity of a shallow circular plate anchor in a two-layer sand bed. For a constant total embedment ratio (H/D), the maximum uplift capacity was found to increase linearly with increasing thickness of a dense lower layer that was overlain by a medium-dense layer, and was found to decrease linearly with increasing thickness of a medium-dense lower layer overlain by a dense layer. When the upper and lower layers were of equal thickness, the maximum uplift capacity was greater for a dense layer overlain by a medium-dense layer than for a medium-dense layer overlain by a dense layer. This implies that a greater proportion of the resistance to uplift is mobilised in the lower layer than the upper layer. The direction of shear band propagation was found to be dependent on the density of the sand, regardless of the layering position. It was steeper in loose sand than dense sand, and changed direction at the boundary between layers. The experimental results and finite-element analysis results were found to be in good agreement.

2.4 Uplift capacity of under-reamed pile foundations in layered sand

Very little experimental research has been carried out on under-reamed piles in layered sand. However, in practice, several field situations require the uplift capacity of under-reamed piles in layered soils. One of the objectives of this research was to address this lack of information.

2.5 Soil-foundation interface friction angle

Relative movement between soil and foundations develops friction along the interface between the two materials. It is expressed as an interface friction angle (δ), the value of which is essential for the design of pile foundations. Numerous experimental studies have been published to determine the interface friction angle between a variety of soils and construction materials using laboratory equipment such as direct shear apparatus (Potyondy, 1961; Acar et al., 1982; Uesugi & Kishida, 1986; Subba Rao et al., 1998) and ring torsion apparatus (Yoshimi & Kishida, 1981a; Yoshimi & Kishida, 1981b). All the publications listed agree that the interface friction angle is dependent on the surface roughness of the construction material. However, there is disagreement on whether the interface friction angle is dependent on the soil density and what the maximum limiting interface friction angle is. An in-depth literature review conducted by Subba Rao et al. (1996) concluded that the discrepancy between the results is due to differences in the manner in which the soil at the interface is prepared. Two categories were identified:

- Type A: The structural material is placed on the free surface of the prepared soil (figure 3(a)). In this case the interface friction angle is found to be independent of the soil density. This is because the surface 'film' does not have the same structural arrangement as the lower layers which are at a specific density (Subba Rao et al., 1996). The maximum limiting interface friction angle is the critical state friction angle of the soil mass.
- Type B: The soil is placed against the material surface which functions as a confined boundary (figure 3(b)). For a given structural material the interface friction angle increases with soil density, and its limiting value is the peak angle of internal friction of the soil.

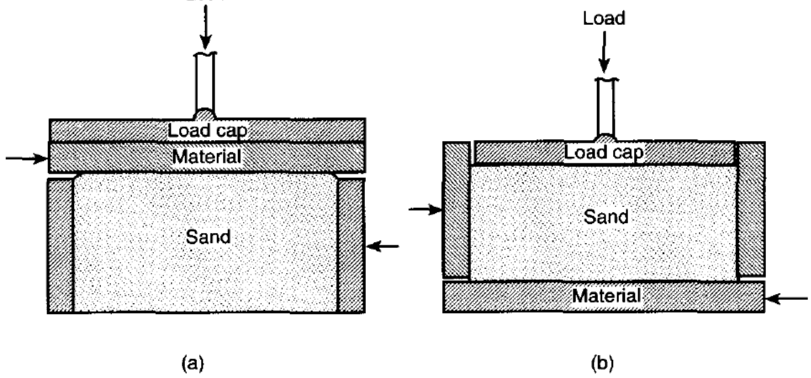

Figure 3: Soil-structure interface preparation: (a) type A, (b) type B (Subba Rao et al. 1996).

The interface friction angle was also found to be dependent on the sand type and mean grain size (Yoshimi & Kishida 1981b; Uesugi & Kishida, 1986; Subba Rao et al., 1998) and the moisture content (Potyondy, 1961).

2.6 Summary

The uplift capacity of plate anchors and under-reamed pile foundations in homogeneous has been observed to increase with increases in embedment depth, anchor diameter, and sand density. However, the magnitude of the uplift capacity of under-reamed pile foundations has been found to be different to that of plate anchors with the same diameter. Several half space model tests have been conducted in homogeneous sand to understand this difference in behaviour. However, there is no agreed upon theory for defining the shape of the failure surface, as is the case for plate anchors.

Several studies have been conducted to investigate the uplift behaviour of plate anchors in layered sand, however very little experimental research has been carried out on under-reamed piles in layered sand. One of the objectives of this research was to address this lack of information.

3. Experimental Equipment and Methodology

The testing procedure for this project involved two types of test:

- standard pullout tests to determine the load-displacement response of smooth under-reamed pile foundations in two-layered sand.
- half space model tests, using PIV analysis, to characterise the failure mechanism geometry for a smooth, 45° under-reamed pile in two-layered sand.

3.1 Test containers

3.1.1 Pullout test container

The pullout tests were performed in a 850 mm diameter, 400 mm deep cylindrical steel container. The container was sufficiently large to allow three piles to be tested per sand pour without interference due to the other piles or the container edges. Pre-drilled holes in the top rim of the container allowed the pile jig to be secured in place.

3.1.2 Half space test container

The half space model tests were performed in a 705 mm long, 300 mm wide and 500 mm deep timber container, with the front face being a detachable, clear perspex window. The size of the container only allowed one pile to be tested per sand pour without interference due to the container edges. The control marker layout adopted by Harris (2014) was used, which was chosen to minimise the number of markers that would overlay and obstruct the mechanism whilst also meeting the PIV software requirements (Harris, 2014).

3.2 Model piles

3.2.1 Model pile specification

The model under-reamed piles used were the same as those used by Hopkins (2013) and Harris (2014). They were machined from blocks of Dural aluminium alloy and had polished, smooth surfaces. The piles were 400 mm in length and 12.7 mm in diameter. The model under-reams had a maximum diameter of 60 mm (figure 4). Under-reams with angles of 0° (plate anchor), 30° and 45° to the horizontal

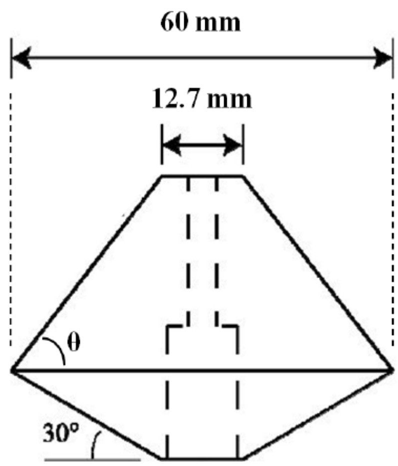

Figure 4: Model under-ream base geometry (Harris, 2014).

were used in the pullout tests. A half space model with an under-ream angle of 45° to the horizontal was used in the half space tests. This pile had a rectangular cross section to enable easier manufacturing, plus a layer of PTFE tape attached to the flat face to provide a low friction interface with the perspex window.

Extension of the pile shaft was ignored due to the low loads applied to the pile. The under-reams were modelled as being perfectly rigid.

3.2.2 Installation of the model piles

It was important to ensure that the piles were installed vertically and not on an incline. For the pullout test model a triangular wooden jig, as used by Harris (2014), was used to ensure that this was achieved. For the half space test model, a plumb bob and spirit level were used as the container geometry made it impractical to use a jig. Silicon grease was applied to the PTFE tape on the flat pile face to prevent sand slipping in-between the pile and the perspex window.

It was important to ensure that the piles were securely held in position during the model preparation. For the pullout test model, the piles were held in position using the previously mentioned jig and screw locks. For the half space test model, the half space pile was held in position using a D-clamp and masking tape.

3.3 Sand

3.3.1 Sand properties

All tests were conducted in dry Hostun HN31 sand. Properties of Hostun HN31 sand used in the Schofield Centre were taken from Mitrani (2006).

Table 1: Properties of Hostun HN31 sand (Mitrani, 2006)

Property	**Value**
e_{max} [-]	1.01
e_{min} [-]	0.555
ϕ_{crit} [°]	33

D_{50} [mm]	0.35

All experimental tests were conducted in sand rather than clay for the following reasons:

- Experimental models are considerably quicker to set up in sand than clay. This meant that more tests could be conducted in the limited time available.
- Installation of the piles in sand is much simpler than in clay, and hence requires less apparatus.

3.3.2 Layering

An initial 100mm layer of sand was poured in all tests to rest the pile bases on.

All layered tests had a dense lower layer and a loose upper layer of sand to model the ground conditions under-reamed piles are usually constructed in. The ratio of the lower layer thickness to total embedment depth (h_2/H) was varied whilst keeping the total embedment depth (H = h_1+h_2) constant at 180mm.

3.3.3 Sand densities

A loose sand relative density of $I_D \approx 20\%$ and a dense sand relative density of $I_D \approx 75\%$ were used throughout this project. These relative densities were obtained by sand pouring or sand compaction.

3.3.4 Sand pouring

A manual sand pourer was used for sand pouring. The drop height and nozzle diameter were chosen to obtain the required relative densities. An oscillatory pouring pattern was used to ensure that each layer was a homogeneous stratum. Once the required depth of sand had been poured, the surface was levelled. The mass of sand poured was used to calculate the relative density achieved.

3.3.5 Sand compaction

Vibro compaction was only used to produce the dense lower layer in the pullout test model. The required mass of sand for the dense layer was placed in the container around the model piles, which were secured in place using the jig. A vibrating table was then used to compact the sand until the height of the layer reduced to the required depth. Sand compaction was not utilised in the half space test model preparation since it was not possible to securely hold the half space model pile in place.

3.3.6 Sand for half space tests

For the half space tests, blue Hostun HN31 sand was mixed with standard Hostun HN31 sand in a 1:10 ratio. This was done to increase the amount of texture in the images used in the PIV analysis and decrease the possibility of tracking failures.

A horizontal layer, approximately 2 mm thick, of blue Hostun HN31 sand was poured adjacent to the perspex window at 30 mm vertical intervals to enable the approximate failure mechanism geometry to be observed without PIV analysis. This technique has previously been used as the sole method to observe the failure mechanism geometry (Balla, 1961; Dickin & Leung, 1992; Sakai & Tanaka, 2007).

3.4 1D Actuator

The uplift force was provided by a 1D actuator attached to the pile head. A shear box was used to control the rate of displacement of the 1D actuator. A constant rate of displacement of 0.1 mm/s was used in all tests. This rate was chosen to ensure no dynamic effects were present and that any settlement of the sand had time to occur during the test.

3.5 Instrumentation

3.5.1 Load measurement

A load cell was used to measure the load applied to the pile. It was positioned between the pile head and the actuator. An 800 N load cell was used for the pullout tests for homogeneous sand. A 1 kN load cell was used for all other tests. This variation in load cells used was due to the 800 N load cell breaking during a test.

The load cell was calibrated before and after each test. Calibration was conducted by replacing the pile with a hanger and incrementally adding known masses within the range of load expected to be measured during the tests. The output voltage was recorded, and used to construct a calibration curve. A linear relationship was obtained between the load applied and the voltage recorded.

3.5.2 Displacement measurement

The pile head displacement was measured using a Linear Variable Differential Transformer (LVDT). The LVDT was positioned above the actuator carriage to ensure it was placed vertically and to ensure a flat measuring surface.

The LVDT was calibrated before and after each test. Calibration was conducted using digital Vernier calipers to impose a known displacement. The output voltage was recorded, and used to construct a calibration curve. A linear relationship was obtained between the displacement imposed and the voltage recorded, with the exception of the extreme ends of travel of the LVDT. Consequently, the LVDT was always positioned to avoid readings in these extreme regions during tests.

3.5.3 Data acquisition

DASYLab 9.0 data acquisition software was used to record data continuously from all instrumentation.

3.6 Camera

A GoPro HERO 3+ Black Edition camera was used to record the half space tests. A 4k resolution video was recorded. This was converted into a series of 4k still images which were used in the PIV analysis.

3.7 Data analysis

3.7.1 Pullout tests

The data from the pullout tests was analysed in MATLAB R2014a.

3.7.2 Half space tests

PIV analysis was conducted in MATLAB R2014a using GeoPIV software developed by White et al. (2003). The patch size used was 12 x 12 pixels at a 12 pixel spacing. This patch size successfully tracked the sand and produced results of a suitable resolution.

3.8 Full experimental setup

The experimental setup for the pullout tests and half space tests are shown in figure 5.

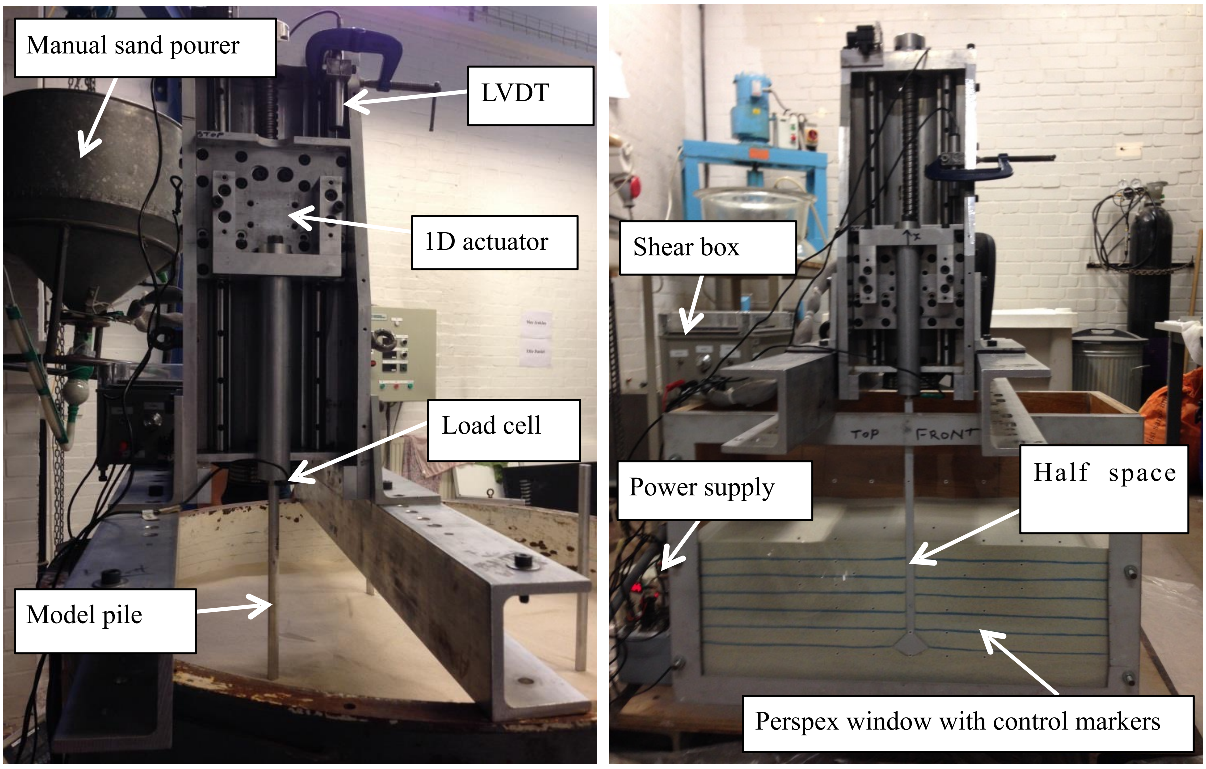

Figure 5: Experimental setup: left: pullout test arrangement, right: half space test arrangement.

3.9 Experimental procedure

3.9.1 Pullout tests

The following procedure was used to conduct all pullout tests. The test container was positioned on the vibrating table for the entire procedure.

1. The mass of sand required for a dense initial 100mm sand layer and the lower dense layer was weighed. An initial 100mm layer was poured, and the sand surface was levelled.
2. The piles were installed using the jig, and secured in position using screw locks. A spirit level was used to ensure that the piles were vertical.
3. The remaining mass of sand from step 1 was poured using the manual sand pourer.
4. The sand was compacted using the vibrating table until the height of the layer reduced to the required depth. The sand surface was then levelled.*
5. The manual sand pourer was used to pour the upper loose sand layer and the mass of sand added was recorded. The sand surface was levelled once the required depth was reached. +

6. The jig was removed. The load cell was connected to the pile head. A plumb bob was used to position the 1D actuator, and it was connected to the load cell. The LVDT was attached to the actuator. All electrical equipment was checked to ensure it was recording correctly.
7. The shear box and power supply were set to the correct settings. DASYLab recording was started, then the 1D actuator was activated. Data was recorded until an approximately constant post-peak capacity was reached.
8. The actuator and all instrumentation were detached and moved onto the next pile. Steps 6 and 7 were repeated.
9. The sand was removed and the tub was cleaned to prepare for the next test.

* This step was not applicable for the homogeneous loose sand test.

+ This step was not applicable for the homogeneous dense sand test.

2. Half space tests

The following procedure was used to conduct all half space tests.

1. The initial 100mm of sand was poured and the sand surface was levelled (there was no specific density requirement for this layer).
2. The half space model pile was installed against the perspex window using a D-clamp and masking tape. A spirit level was used to ensure that the pile was vertical.
3. The manual sand pourer was used to pour the dense lower layer and loose upper layer. Every 30mm, an approximately 2mm thick horizontal layer of blue HN31 Hostun sand was poured adjacent to the perspex window. The masking tape was removed sequentially during the sand pouring. The sand surface was levelled once the required depth was reached.
4. The D-clamp was removed. The load cell was connected to the pile head. A plumb bob was used to position the 1D actuator, and it was connected to the load cell. The LVDT was attached to the actuator. All electrical equipment was checked to ensure it was recording correctly.
5. The shear box and power supply were set to the correct settings. DASYLab recording was started, the camera recording was started, then the 1D actuator was activated. Data was recorded until an approximately constant post-peak capacity was reached.

6. The sand was removed and the tub was cleaned to prepare for the next test.

3.10 Tests performed

The total embedment depth (H) in all tests was 180mm.

3.10.1 Pullout tests

The following pullout tests were conducted.

Table 2: Details of pullout tests performed

Test name	**Aim**	**h_2/H**	**Relative density I_D [%]**		**Under-ream angles [°]**
			Upper layer h_1	**Lower layer h_2**	
FEH1	To determine the load-displacement characteristics and capacity of under-reamed piles in loose sand	0	14	-	0 30 45
FEH2	To determine the load-displacement characteristics and capacity of under-reamed piles in dense sand	1	-	75	0 30* 45
FEH3	To determine the load-displacement characteristics and capacity of under-reamed piles in two-layered sand	1/2	21	75	0 30 45
FEH4	To determine the load-displacement characteristics and capacity of under-reamed piles in two-layered sand	1/3	24	75	0 30 45
FEH5	To determine the load-displacement characteristics and capacity of under-reamed piles in two-layered sand	2/3	18	75	0 30 45

* The load cell broke during this test; therefore there is no test data available.

2. Half space tests

The following half space tests were conducted.

Table 3: Details of half space tests performed

Test name	**Aim**	**h_2/H**	**Relative density I_D [%]**		**Under-ream angle [°]**
			Upper layer h_1	**Lower layer h_2**	

FEH6	To determine the failure mechanism for a 45° under-reamed pile in two-layered sand	1/3	24	74	45
FEH7	To determine the failure mechanism for a 45° under-reamed pile in two-layered sand	2/3	20	68	45
FEH8	To determine the failure mechanism for a 45° under-reamed pile in two-layered sand	1/2	20	72	45

3.11 Experimental accuracy

3.11.1 Pullout tests

The main sources of experimental inaccuracy were the orientation of the model piles and the load cell. Care was taken when installing the piles to ensure that they were vertical and not at an incline (see section 3.2.2). The load cell used was very sensitive to applied moment loading, so measures were taken to ensure the load transmitted was purely axial. A spirit level was used to ensure that the 1D actuator was placed flat onto the test container and a plumb bob was used to perfectly align the actuator above the pile head. The connection between the pile head, load cell and the actuator was assembled carefully.

3.11.2 Half space tests

As with the pullout tests, the orientation of the model pile was a source of experimental inaccuracy in the half space tests. Care was taken when installing the piles to ensure that they were vertical and not on an incline (see sections 3.2.2 and 3.11.1).

4. Uplift Behaviour in a Uniform Sand Bed

The non-dimensionalised load-displacement curves from the pullout tests are presented on graphs with the normalised pullout capacity $N = \frac{Q}{\gamma' AH}$ plotted against normalised displacement y/D.

4.1 Experimental results

The non-dimensionalised load-displacement curves for all under-reamed piles tested in a homogeneous sand bed closely follow the expected behaviour of sand subjected to simple shear (figure 6). In dense sand a well defined peak uplift capacity is observed, with a significant post-peak reduction in capacity, whereas in loose sand no such reduction is observed.

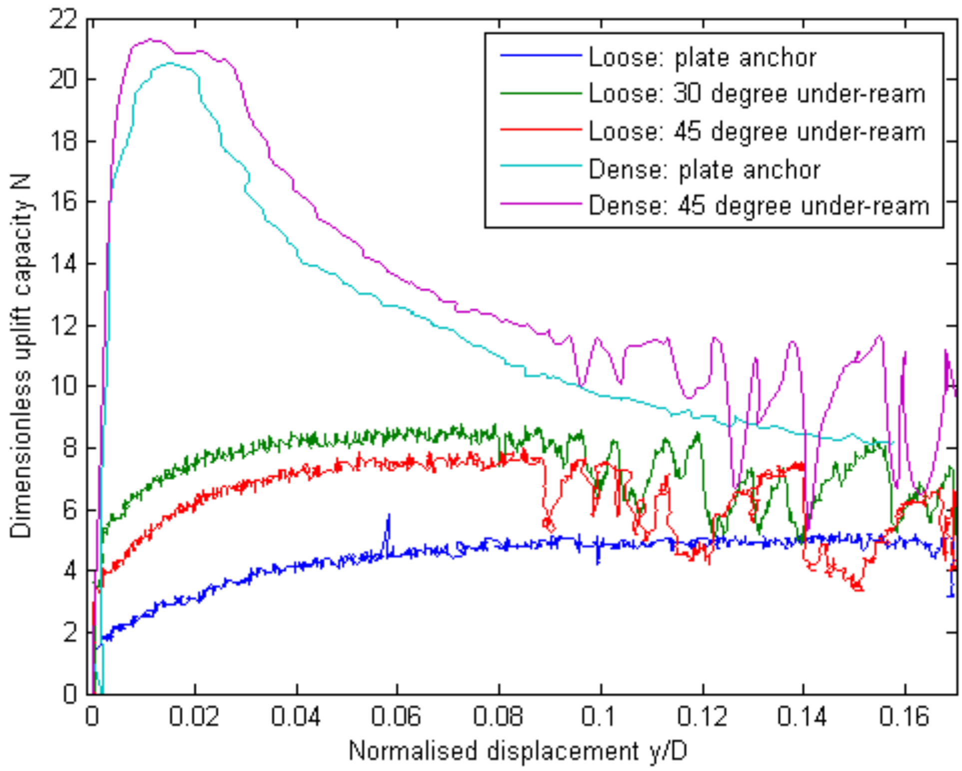

Figure 6: Non-dimensionalised load-displacement curves for under-reamed pile foundations in homogenous sand.

The capacity of the under-reamed piles is much greater in homogeneous dense sand than homogeneous loose sand and the normalised displacement at failure is significantly less (figure 6). The 30° under-reamed pile has the highest capacity of the under-reamed piles tested, with the plate anchor having the lowest. Fluctuations in load at large normalised displacements occur for the 30° and 45° degree under-reamed piles, but not for the plate anchor.

4.2 Comparison to literature

The load-displacement behaviour observed in this project is in agreement with that previously observed for plate anchors in homogeneous sand (Murray & Geddes, 1987; Sakai & Tanaka, 2007; Hopkins, 2013; Harris & Madabhushi, 2015) and under-reamed pile foundations in homogeneous sand (Dickin & Leung, 1990; Hopkins, 2013; Harris & Madabhushi, 2015). In contrast, it is not in agreement with the results observed by Ilamparuthi et al. (2002) for plate anchors in homogeneous sand which found the load-displacement behaviour of circular plate anchors to be independent of the density of the sand, but to be dependent on whether the anchor was shallow or deep.

There is a discrepancy between the results obtained in this present project and those obtained in the centrifuge model test programme conducted by Dickin & Leung (1992). Dickin & Leung (1992) found that, in both homogeneous loose and dense sand, the normalised peak uplift capacity was greater for plate anchors than for under-reamed piles, with the ratio between the two essentially being independent of soil unit weight. It is possible that this discrepancy is due to scale effects and emphasises that small scale model tests conducted at 1-g should not be used to predict the load response or settlement for fully sized piles.

Fluctuations in load at large normalised displacements were observed to occur for the 30° and 45° under-reamed piles, but not for the plate anchor (figure 6). This behaviour has previously been observed for under-reamed piles (Dickin & Leung, 1992; Harris & Madabhushi, 2015), and for plate anchors (Rowe & Davis, 1982; Ilamparuthi et al., 2002). The model tests which observed fluctuations in load at large displacements for plate anchors were conducted using significantly larger model piles than were used in the present project, this being likely to be the reason behind the fact that both Harris & Madabhushi (2015) and the present project did not observe this behaviour for plate anchors. The fluctuations in load at large displacements are due to soil arching (Ilamparuthi et al., 2002) whereby the sand around the base of the foundation forms an arch providing resistance, but is unstable due to the large cavity underneath the pile. As a result, the sand collapses to fill the space, causing the pile load to drop. A new arch is then formed and the cycle then repeats itself.

5. Influence of Dense Layer Thickness

5.1 Experimental results

For all the two-layered tests conducted, the total embedment depth was 180mm, which was equal to three times the maximum diameter of the model under-reamed piles used.

The non-dimensionalised load-displacement curves for the three two-layered sand tests (figures 7-9) show a peak capacity followed by a post-peak reduction in capacity. The normalised displacement at peak capacity is similar for all two-layered configurations, and lies between that found in homogeneous dense and loose sand. The initial stiffness response of the piles in two-layered sand is the same as for the homogeneous dense sand test. The presence of the loose upper layer reduces the stiffness response as peak capacity is approached and greatly reduces the peak uplift capacity of the piles. In general, the greater the ratio h_2/H (equating to a greater depth of dense lower layer) the greater the dimensionless peak uplift capacity, with the exception that the dimensionless peak uplift capacity for $h_2/H = 1/3$ is greater than that for $h_2/H = 1/2$.

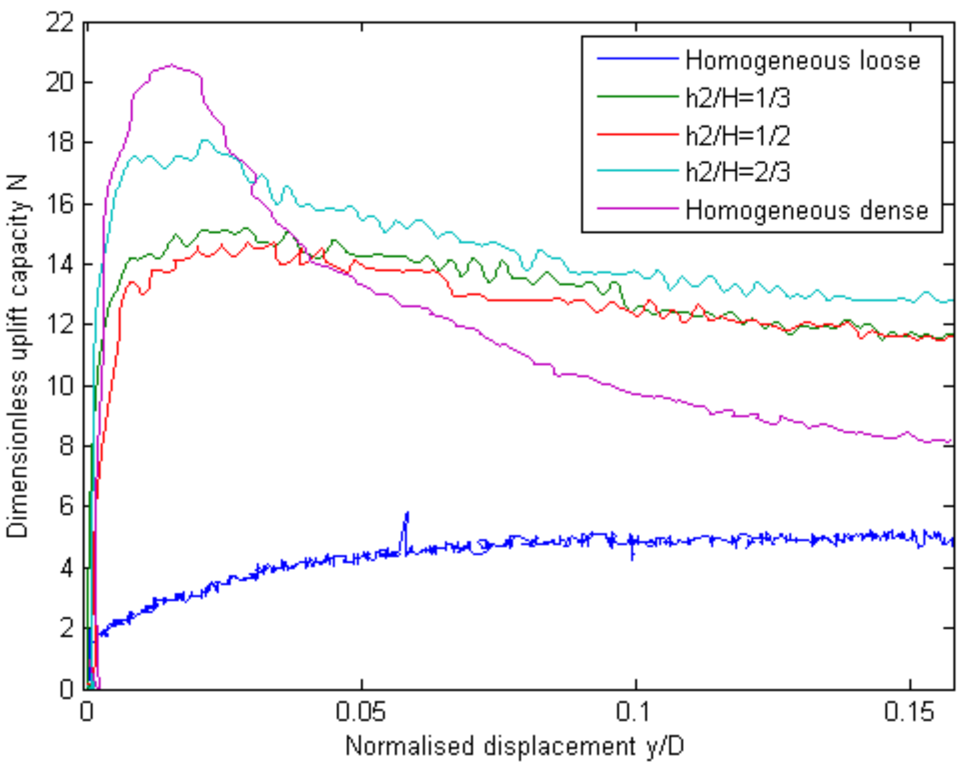

Figure 7: Non-dimensionalised load-displacement curves for plate anchor.

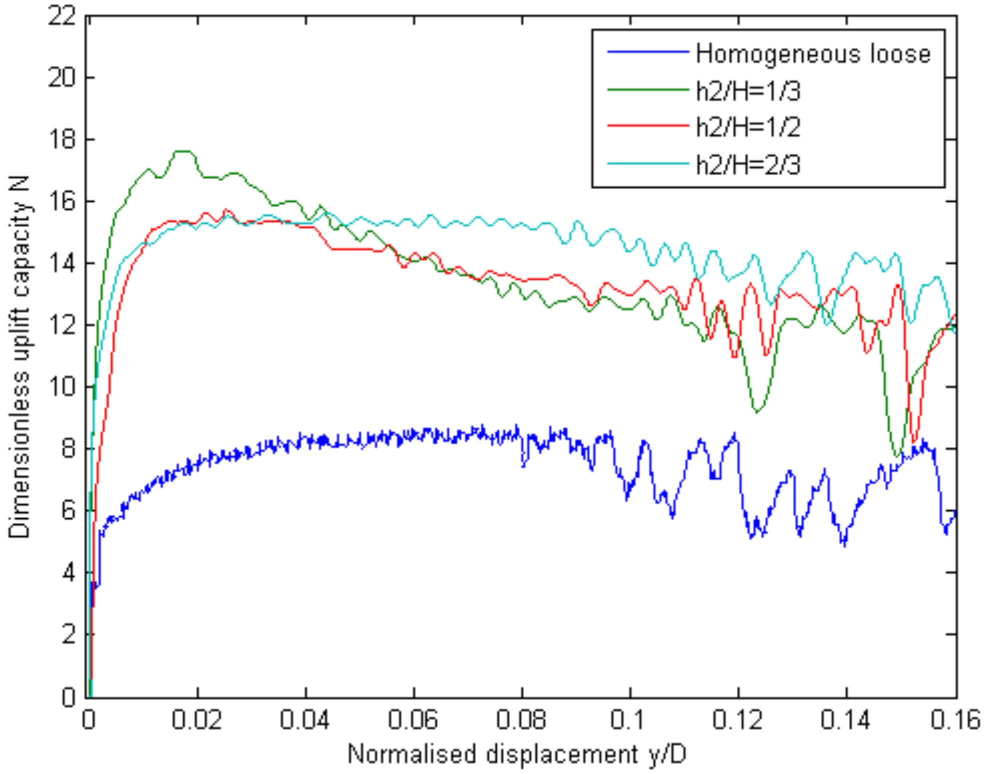

Figure 8: Non-dimensionalised load-displacement curves for 30° under-reamed pile.

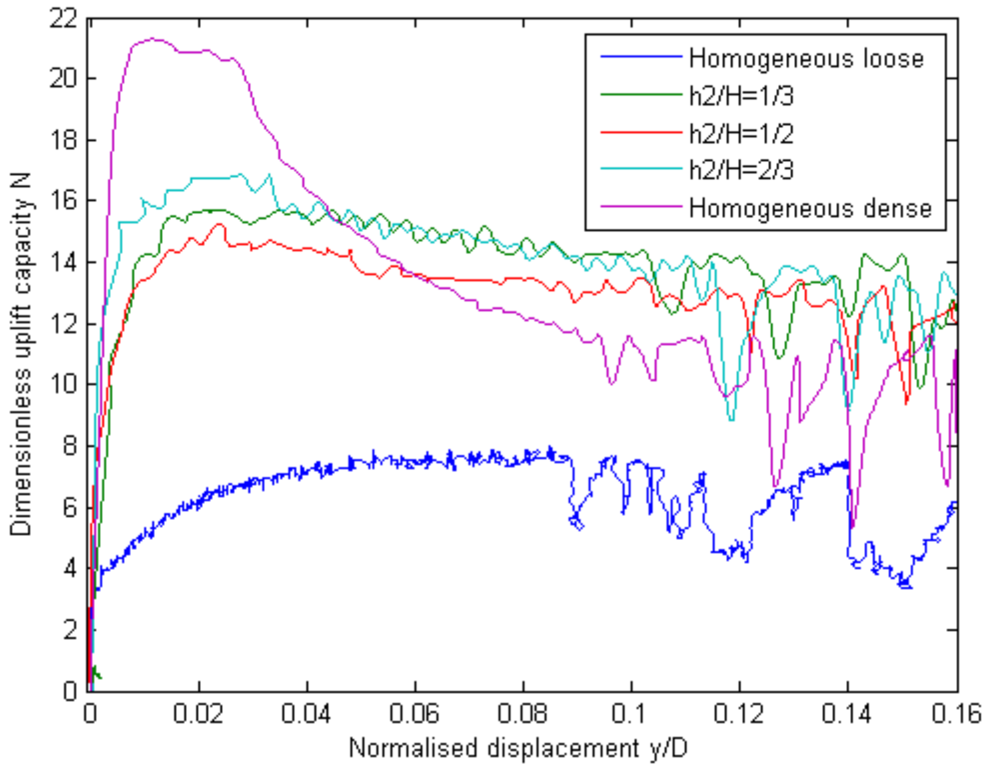

Figure 9: Non-dimensionalised load-displacement curves for 45° under-reamed pile.

At large

normalised displacements, the dimensionless post-peak capacities of the under-reamed pile foundations are greater in all three of the two-layered sand tests than in both the homogeneous loose and homogeneous dense sand tests (homogeneous dense sand test data is not available for the 30° under-reamed pile). Fluctuations in load at large normalised displacements were observed for all layering configurations for the 30° and 45° under-reamed pile foundations (figures 8 and 9), but not for the plate anchor (figure 7).

The peak uplift capacities of the three model piles tested are very similar for a given layering configuration, with the pile with the greatest peak capacity varying between the different layering configurations (figure 10). An approximately linear relationship is observed between the peak uplift capacity and the ratio of lower layer thickness to the total embedment.

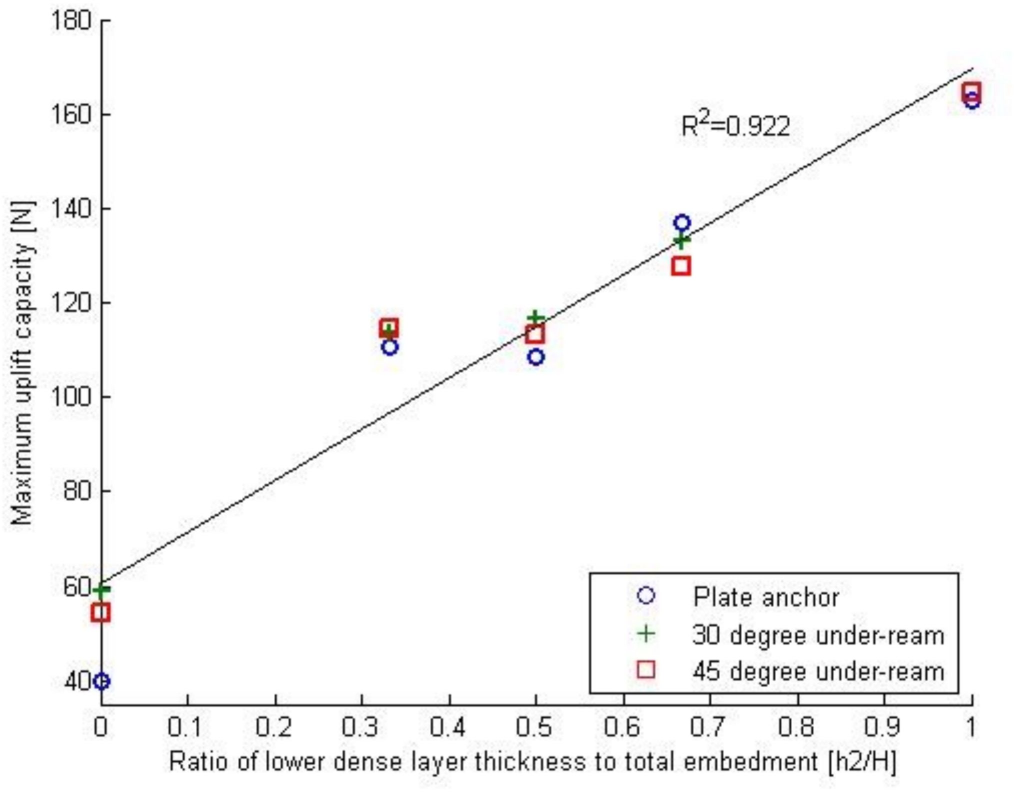

Figure 10: Relationship between maximum uplift capacity and dense lower layer thickness.

2. Comparison to literature on plate anchors in two-layered sand

A peak capacity followed by a post-peak reduction in capacity observed in the load-displacement curves for under-reamed pile foundations in two-layered sand in this project (figures 7-9) had previously been observed for plate anchors in two-layered sand (Bouazza & Finlay, 1990; Sakai & Tanaka, 2007). The tests conducted at 1-g by Sakai & Tanaka (2007) found that for a constant total embedment, the maximum uplift resistance increased linearly with increasing thickness of a dense lower layer which was overlain by a medium-dense layer. A very similar relationship was observed in this project for a dense lower layer overlain by a loose upper layer (figure 10). These two similarities between the uplift behaviour of under-reamed piles and plate anchors in two-layered sand imply that the two involve similar failure mechanisms.

5.3 Failure mechanism characterisation

Three half space tests were conducted using a half space model 45° under-reamed pile foundation in the three two-layered sand configurations used in the pullout tests. The total embedment depth was kept constant at 180mm. The small strain, peak capacity and post-peak failure mechanisms were compared. The small strain failure mechanism corresponds to an applied uplift equal to half the peak uplift capacity, the peak capacity failure mechanism corresponds to when the maximum uplift capacity was obtained and the post-peak failure mechanism corresponds to the displacement where an approximately constant post-peak uplift capacity was reached.

The sand displacement vectors from the PIV analyses of these tests are plotted over an image of the initial position of the under-reamed pile (figures 11-13). The vectors are scaled up for clarity. Wild vectors caused by tracking failures have been removed. The loose upper layer is shown as being lighter than the dense lower layer. The thin horizontal blue layers of sand are at 30 mm intervals vertically.

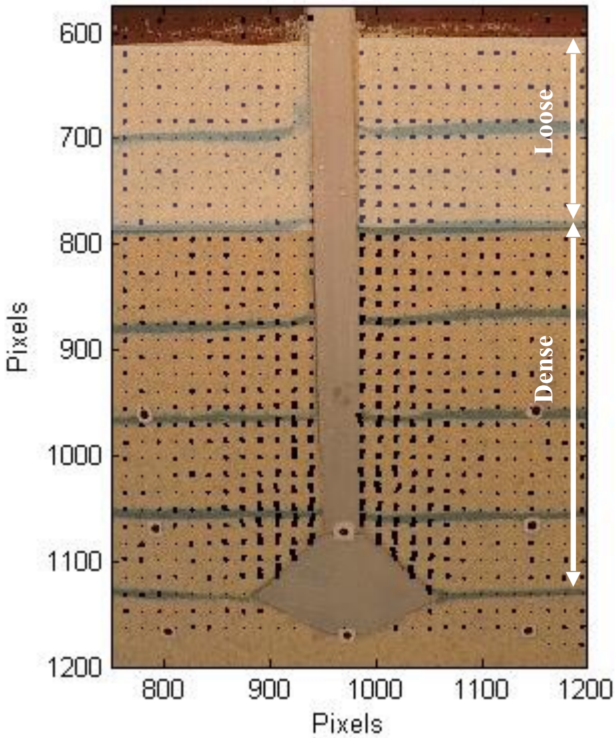

(a)

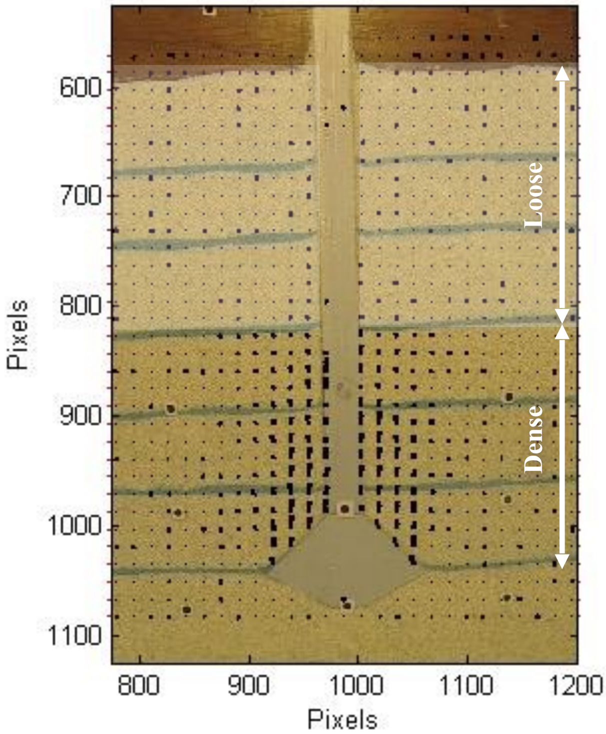

(b)

Figure 11: PIV analysis of small strain failure mechanisms with vectors scaled up by factor of 20: (a) $h_2/H = 2/3$: (b) h_2/H =

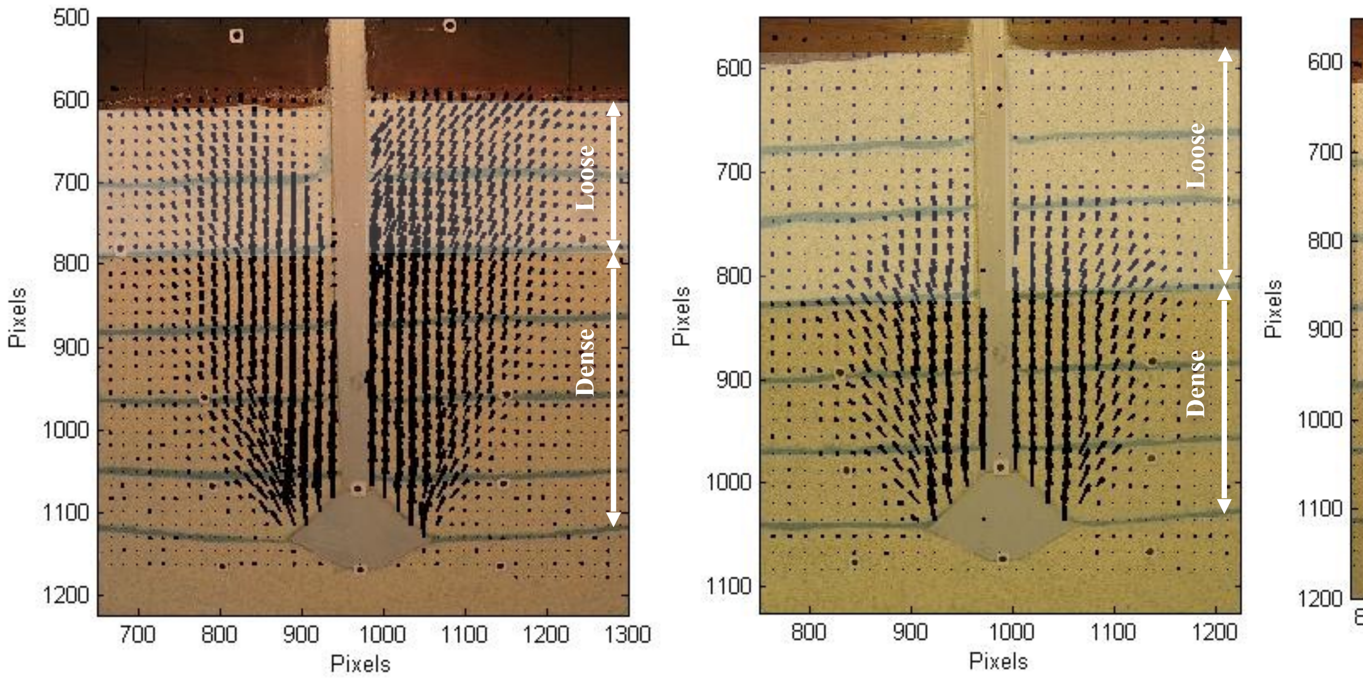

(a) (b)

Figure 12: PIV analysis of peak capacity failure mechanisms with vectors scaled up by a factor of 10: (a) $h_2/H = 2/3$: (b

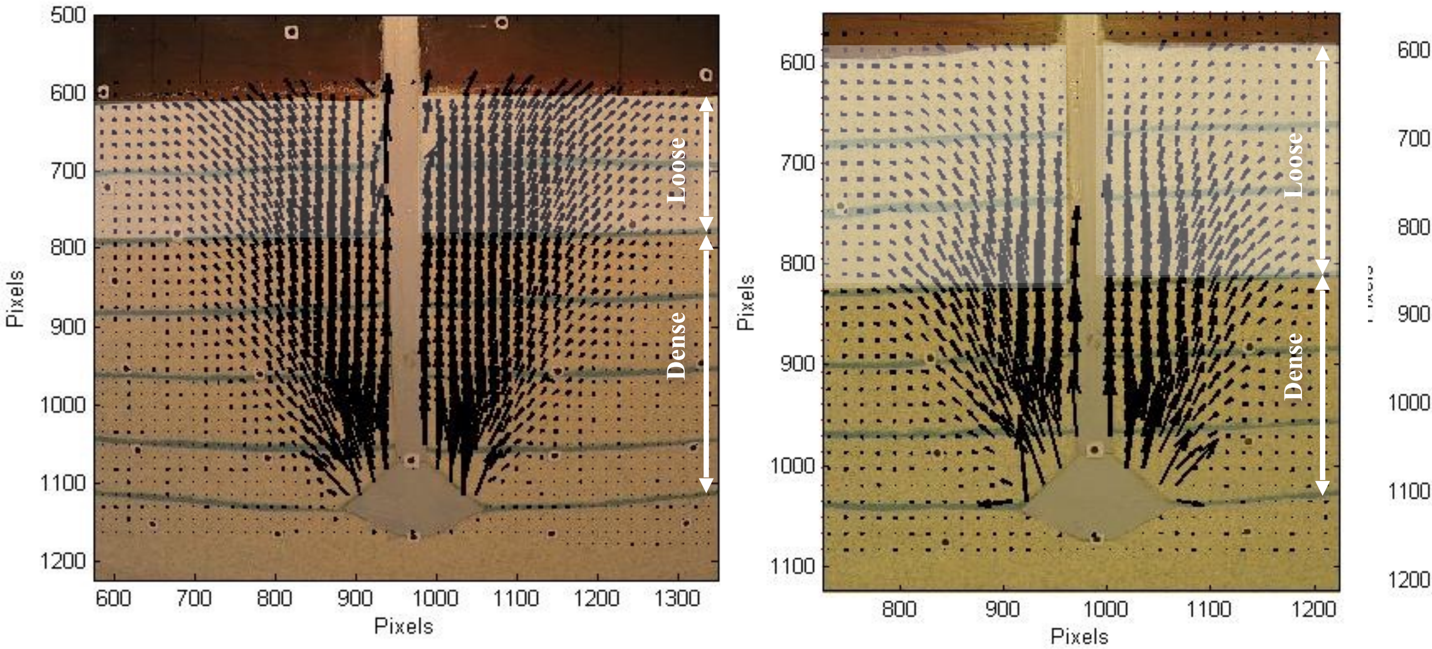

(a) (b)

Figure 13: PIV analysis of post-peak failure mechanisms with vectors scaled up a by a factor of 5: (a) $h_2/H = 2/3$: (b) $h_2/H = 1/$

F i o n a

Hughes
5.3.1 Small strain failure mechanisms

The small strain failure mechanisms are very similar for all three two-layered configurations tested (figure 11), hence explaining the same initial stiffness response for the under-reamed piles in the different layering configurations (figures 7-9). At small strains, caused by small imposed displacements, resistance is only mobilised in the lower dense layer and not in the upper loose layer (figure 11). This is evident as displacement vectors are only observed in the lower layer, and extend to approximately the dense-loose sand boundary. These displacements are only observed in the column of sand vertically above the under-ream and no rotation of the vectors is observed.

5.3.2 Peak capacity failure mechanisms

At peak capacity the dense lower layer is seen to mobilise large displacements (figure 12). If only a shallow layer of loose sand in present (figure 12 (a)), all the strains are mobilised in the loose layer and the displacements reach the ground surface. However, if a sufficiently thick layer of loose sand is present, the displacements are prevented from reaching the ground surface by local compaction of the loose sand layer (figures 12(b) and (c)). Mobilisation of resistance within the loose upper layer, which occurs for an uplift capacity between half the peak capacity (figure 11) and the peak capacity (figure 12), reduces the stiffness of the under-ream piles as observed in the pullout tests (figures 7-9).

For all three tests conducted, in the lower dense layer there is very little variation in vector magnitude in the column of soil vertically above the under-ream (figure 12). This indicates that very little sand contraction occurred, which is what would be expected in dense sand. The column therefore moved almost as a rigid block. Away from this column, the dense sand is seen to displace by a smaller, constant magnitude and at an angle to the vertical, forming a cone. The angle of the edge of the cone is seen to be approximately the same across the three tests conducted, with a mean value of approximately 67° to the horizontal. The vectors immediately above the under-ream appear to be approximately vertical. For all three tests conducted there is no movement observed in the sand below the base of the pile.

F i o n a

Hughes
The cone failure mechanism in the dense sand is observed to extend into the loose upper layer, but then rounds off to form a “balloon” shaped mechanism in the loose sand (figure 12). As the failure mechanism passes through the dense-loose sand boundary, the vector magnitude decreases and continues to decrease as the distance above the boundary increases, indicating that the loose sand contracts. This is expected in loose sand, as loose sand contracts when sheared.

For the layering configurations $h_2/H = 1/2$ and $h_2/H = 1/3$ (figures 12 (b) and (c)), the inclination of the vectors to the horizontal outside of the column immediately above the under-ream base is seen to noticeably increase across the dense-loose sand boundary, with the change in angle greater the smaller the depth of the dense lower layer. For the layering configuration with $h_2/H = 2/3$ (figure 12 (a)), there is no noticeable change in inclination of the vectors across the dense-loose boundary. However, the inclination of the vectors to the horizontal is seen to significantly decrease as the failure mechanism approaches the ground surface.

5.3.3 Post-peak failure mechanisms

The post-peak failure mechanisms are fully developed. All the strains are mobilised in the loose upper layer and the displacements reach the ground surface for all layering configurations tested (figure 13). Consequently, there is a greater volume of soil within the failure mechanisms at post-peak capacity (figure 13) than at peak capacity (figure 12).

The mean inclination of the soil displacement vectors immediately above the under-ream across all three tests is approximately 14° to the vertical. For all three tests conducted, the inclination of the vectors to the horizontal is seen to significantly decrease between 60mm below the ground surface and the ground surface itself, implying that this sand is being displaced horizontally to accommodate the under-ream and sand which is being uplifted.

5.4 Comparison to literature

5.4.1 Failure mechanism characterisation

In model tests conducted at 1-g and finite-element analysis of plate anchors in two-layered sand, Sakai & Tanaka (2007) observed the direction of shear band propagation to change at the boundary between layers of different densities, with the angle to the horizontal greater in loose sand than dense sand. This behaviour was also observed in the present project for the layering configurations $h_2/H = 1/2$ and $h_2/H = 1/3$. Sakai & Tanaka (2007) did not use PIV analysis and so it is difficult to make any further comparisons.

The failure mechanisms at peak capacity in both the loose and dense layers are similar to those observed by Harris & Madabhushi (2015) for 45° under-reamed piles in homogeneous loose and dense sand respectively. The mean angle of the edge of the cone failure mechanism in the dense layer in the present research was found to be approximately the same as that observed by Harris & Madabhushi (2015) for a plate anchor and 45° under-reamed pile, which they noted was approximately equal to $90° - \phi/2$ to the horizontal. Dickin & Leung (1992) also observed a roughly conical rupture plane for a 45° under-reamed pile in homogeneous dense sand. However, in contrast to the results of the present project and that of Harris & Madabhushi (2015), Dickin & Leung (1992) found that in homogeneous loose sand relative movement was restricted to the under-ream-sand interface, with no failure in the sand mass. Their tests did not involve PIV analysis; therefore it is possible that displacements occurred in the loose sand but were not identified by the horizontal dyed layers.

At peak capacity, Harris & Madabhushi (2015) observed the soil displacement vectors immediately above a plate anchor to be vertical in both homogeneous loose and homogeneous dense sand. For a 45° under-reamed pile they observed them to have an mean inclination of approximately 12° and 8° to the vertical in homogeneous loose and dense sand respectively, this being significantly less than the angle of the under-ream surface to the vertical (45°). In the present project the soil displacement vectors were observed to be approximately vertical and not at an angle to the under-ream. At peak capacity, smooth, 45° under-reamed piles therefore behave like plate anchors in two-layered sand, hence explaining the similar peak uplift capacities obtained for the plate anchor and the two under-reamed piles tested in the pullout tests (figure 10).

Using experimental test results from model tests conducted at 1-g, Ilamparuthi et al. (2002) suggested values for the critical embedment ratio $(H/D)_{critical}$ for plate anchors in homogeneous sand to be 4.8 and 6.8 for loose and dense sand respectively. The vertical height of the failure mechanisms observed in the present project were observed to be greater for dense sand than loose sand, in agreement with the trend proposed by Ilamparuthi et al. (2002). However, for H/D = 3 used in the present project, not all of the failure mechanisms extended to the soil surface, which is what would have been expected from the results of Ilamparuthi et al. (2002). The model tests conducted in homogeneous sand by Harris & Madabhushi (2015) found that for a plate anchor and 45° under-reamed pile, when H/D ≈ 3 the failure mechanism in dense sand extended to the soil surface, but did not in loose sand, and that the vertical height of the failure mechanism in loose sand was less for the 45° under-reamed pile than the plate anchor. The vertical height of the failure mechanism, and consequently the critical embedment depth, is therefore dependent on the density of the sand, the layering configuration and the under-ream angle.

The numerical study performed by Merifield & Sloan (2006) observed that there was no plastic shearing or flow below a plate anchor in homogeneous sand at peak capacity. The PIV analysis of the half space model tests in the present project also found that there was no displacement of the soil below a 45° under-reamed pile at peak capacity in any of the layering configurations tested (figure 12).

5.4.2 Surface roughness

The minimum value of the surface roughness of aluminium presented by Yoshimi & Kishida (1981b) is R=10μm. The plot of interface friction angle against normalised roughness presented by Subba Rao et al. (1998) was used to determine the interface friction angle between the model under-ream and Hostun HN31 sand. The properties of Hostun HN31 sand used in this project (table 1) are most similar to that of sand 5 used by Subba Rao et al. (1998). The model preparation for this project falls into the type B category identified by

F i o n a

Hughes
Subba Rao et al. (1996), where soil is placed against the material surface which functions as a confined boundary (see section 2.5). The normalised roughness is given by:

$$R_n = \frac{R}{D_{50}} = 0.03$$

Therefore the interface friction angle between the model under-ream and Hostun HN31 sand is approximately δ=17°.

The mean inclination of the soil displacement vectors to the vertical immediately above the under-ream at post-peak capacity (figure 13) is therefore approximately equal to the interface friction angle.

F i o n a
Hughes

6. Theoretical Predictions

Lower and upper bound theoretical predictions of the capacity of foundations assume that the failure mechanism is fully developed. This section will therefore look at the theoretical predictions of, and the comparison to the experimental data for, the post-peak uplift capacity of under-reamed pile foundations.

6 . 1 Lower bound solution

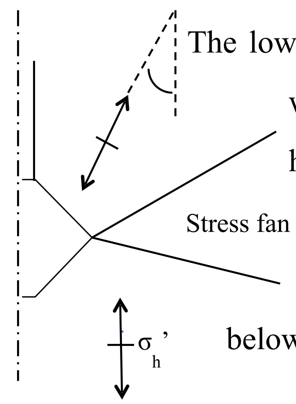

Figure 14: Assumed stress field around the under-ream.

The lower bound solution for the bearing capacity of a strip footing on weightless Coulomb soil under inclined loading (Bolton, 1979) has been modified to calculate the post-peak uplift capacity due to the surcharge acting on the under-ream. The assumed stress field around the under-ream is shown in figure 14. The soil below the pile base is assumed to be in a state of active failure and the soil above the under-ream is assumed to be in a state of passive failure. A log spiral stress fan joins these two regions, and is assumed to rotate the principal stress direction by an angle equal to that of the interface friction angle. Mohr's circles of stress are used to relate the stresses within these regions (figure 15).

The following equations were used to calculate the vertical stress acting on the under-ream due to the surcharge:

$$\sigma_h' = \left(\frac{1-\sin\phi}{1+\sin\phi}\right)\sigma_v' = K_a\sigma_v'$$

where K_a is the active earth pressure coefficient.

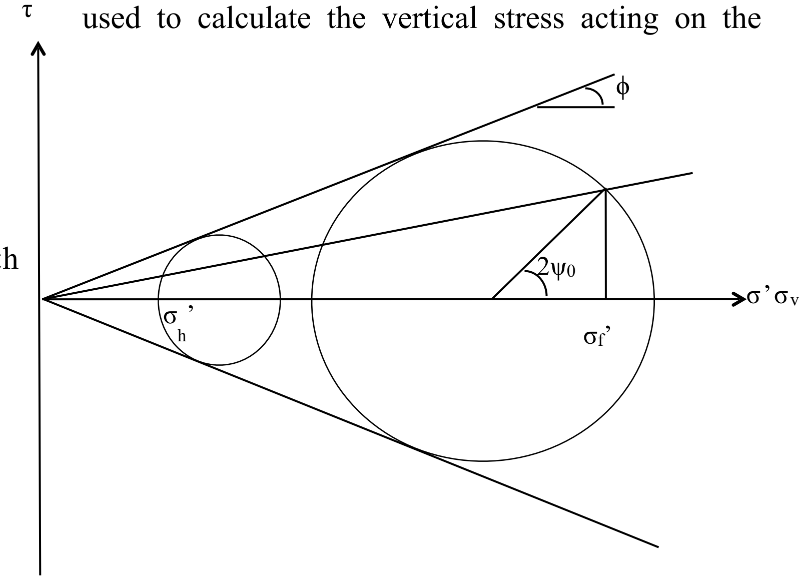

Figure 15: Mohr's circles of stress.

F i o n a

Hughes

$$\sigma_f' = \sigma_h' s_q \frac{(1+\sin\phi\cos 2\psi_0)}{1-\sin\phi}\exp\left[2\tan\phi\left(\frac{\pi}{2}-\psi_0\right)\right]$$

where s_q is the shape factor, and for a circular foundation is give by

$$s_q = 1 + \sin\phi$$

and where the angle of rotation of the principal stress direction is assumed to be equal to the interface friction angle

$$\psi_0 = \delta$$

This lower bound solution does not distinguish between under-reamed piles with different under-ream angles.

6.2 Upper bound solution proposed by Kumar (2003)

Using a computer programme written in FORTRAN, Kumar (2003) used the upper bound theory of limit analysis to find the vertical uplift capacity of circular plate anchors in two-layered sand. The sand was assumed to follow an associated flow rule. Consequently, when there is no surface surcharge present, the only work done within this upper bound solution is against self-weight. The critical collapse mechanism was found to involve the entire soil wedge lying above the anchor to move as a single rigid block, with the same velocity as the anchor itself (figure 16).

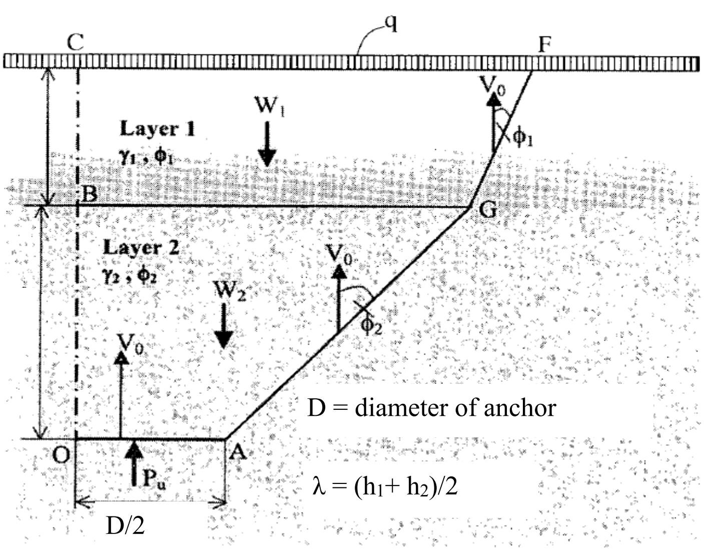

Figure 16: Critical collapse mechanism (after Kumar (2003)).

The upper bound solution proposed by Kumar (2003) is therefore equal to the self-weight of the sand within a failure mechanism bound by linear rupture lines inclined to the vertical at an angle equal to the internal soil friction angle (ϕ) for the corresponding layer (figure 16).

6.3 Comparison to literature and experimental test results

The lower bound theoretical prediction of the post-peak uplift capacity is less than the post-peak uplift capacity of the 45° under-reamed pile observed in the pullout tests (figure 17). This was expected since the stress field used in the lower bound theoretical prediction (figure 14) satisfies equilibrium and boundary conditions without exceeding yield, so collapse cannot occur. There is close agreement between the lower bound solution and the experimental test result in homogeneous loose sand ($h_2/H = 0$).

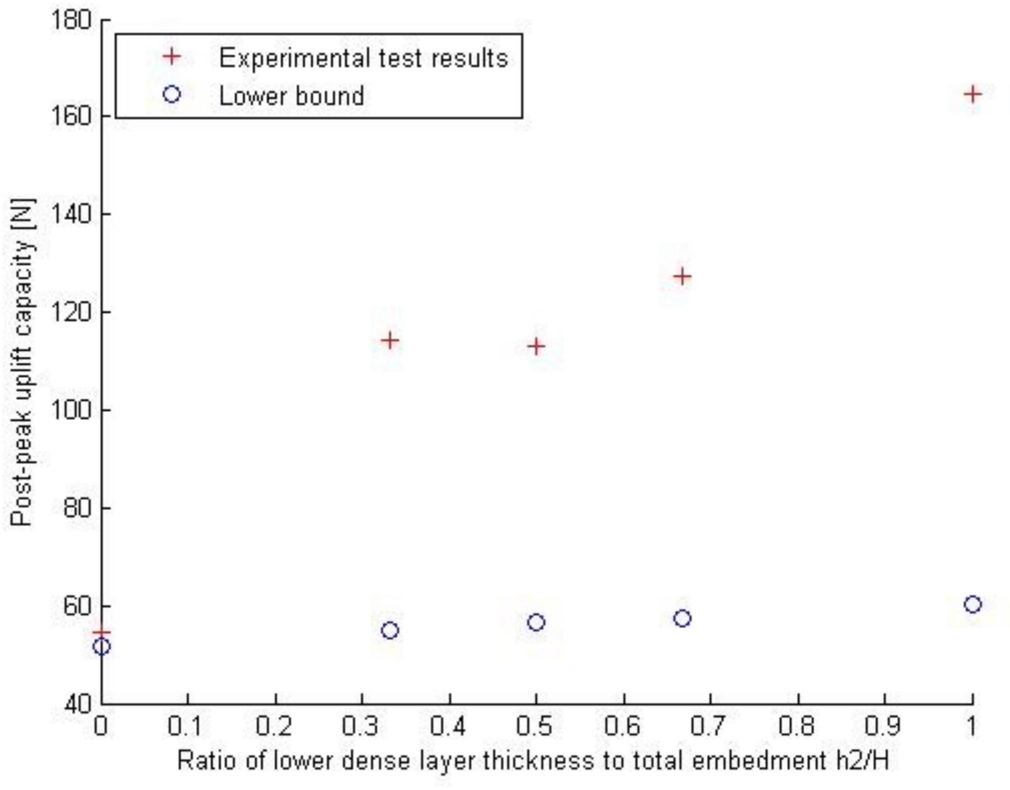

Figure 17: Relationship between post-peak uplift capacity and dense lower layer thickness.

With the exception of homogeneous loose sand ($h_2/H = 0$), the upper bound solution proposed by Kumar (2003) underestimates the experimental post-peak uplift capacity of the under-reamed piles tested (figure 18). This unexpected observation is believed to be due to the incorrect assumption that normality is obeyed. From the half space model tests conducted it is evident that

Fiona Hughes

normality is not obeyed since the angle of the edges of the failure mechanisms to the vertical was not equal to the friction angle (figure 13). The assumption that normality is obeyed imposes an uplift mechanism which involves a far greater volume of sand than has be observed in the half space tests (figure 19) and requires that there is no frictional resistance along the failure surface since there is no internal energy dissipation. An

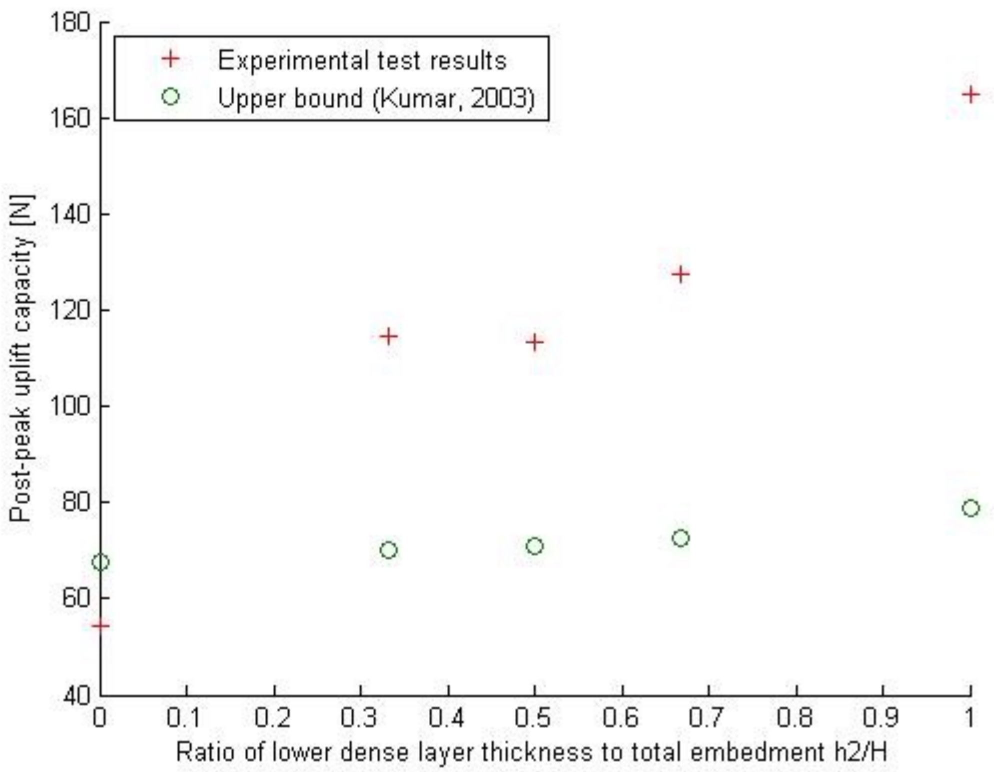

Figure 18: Relationship between post-peak uplift capacity and dense lower layer thickness.

additional discrepancy between the failure mechanism observed in the present project and that obtained by Kumar (2003) is that the two layers were not observed to move as rigid blocks with the same velocity, since the displacement vector magnitudes and directions are not the same within each layer and between the two layers (figure 13). Consequently, the upper bound solution proposed by Kumar (2003) is not a correct upper bound for the under-reamed pile tests conducted in this present project.

In the tests conducted in this project, the ignored resistance due to friction along the failure surfaces appears to be greater than the resistance provided by the volume of sand which is

F i o n a

Hughes
incorrectly assumed to be within the failure mechanism. The difference between the magnitudes of these two inaccuracies appears to increase as the ratio of lower dense layer thickness to total embedment (h_2/H) increases (figure 18).

In contrast, the upper bound solution proposed by Kumar (2003) is a little higher than, but in reasonable agreement with, the experimental results of Bouazza & Finlay (1990) for shallow plate anchors at peak capacity (Kumar, 2003). In this case the resistance due to friction along the failure surfaces appears to be less than the resistance provided by the volume of sand which is incorrectly assumed to be within the failure mechanism.

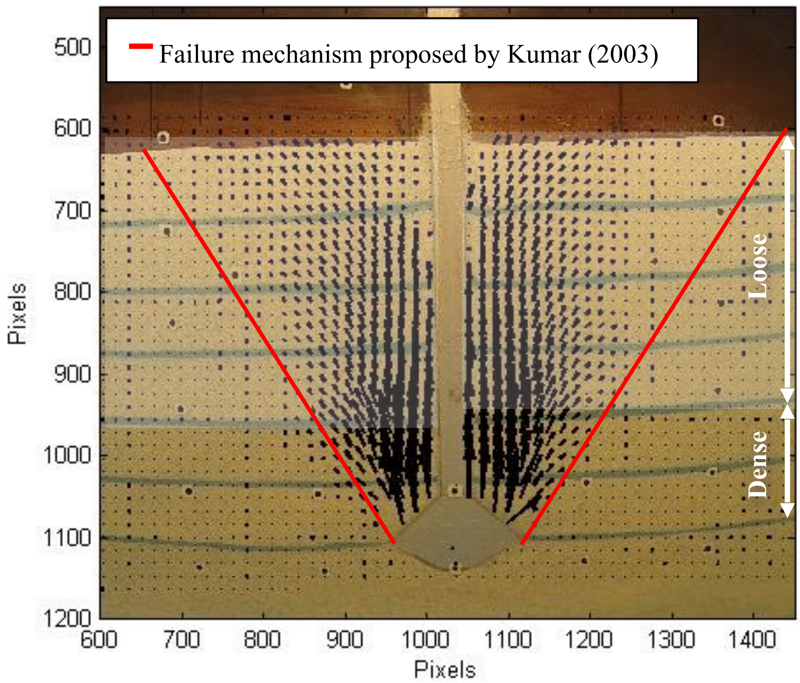

Figure 19: Comparison between the post-peak failure mechanism observed for $h_2/H = 1/3$ and that proposed by Kumar (2003).

F i o n a

Hughes

7. Conclusions

From the pullout tests conducted in this project, the load-displacement behaviour of under-reamed piles in two-layered sand was found to display a peak capacity followed by a post-peak reduction in capacity. The normalised displacement at peak capacity was similar for all two-layered configurations tested and lies between that found in homogeneous dense and loose sand. The initial stiffness response of the piles in two-layered sand was the same as for homogeneous dense sand. However, the presence of the loose upper layer was found to both reduce the stiffness response as peak capacity was approached and also significantly reduce the peak uplift capacity of the piles. An approximately linear relationship was observed between peak uplift capacity and the ratio of lower layer thickness to the total embedment.

PIV analysis of the half space model tests conducted in this project was used to characterise the failure mechanism geometry for a smooth, 45° under-reamed pile in two-layered sand. At small strains, resistance was observed to only be mobilised in the lower dense layer. The small strain failure mechanisms were very similar for all three two-layered sand configurations tested, hence explaining the same initial stiffness response for the under-reamed piles in the different layering configurations. The subsequent mobilisation of resistance within the loose upper layer, which occurred before the peak capacity was obtained, is believed to cause the observed reduction in the stiffness response as peak capacity was approached.

In contrast, at peak capacity the layering configuration had a significant effect on the failure mechanism mobilised. At peak capacity the dense lower layer was seen to mobilise large displacements. If only a shallow upper layer of loose sand was present, all the strains were mobilised in the loose layer and the displacements reached the ground surface. However, if a sufficiently thick upper layer of loose sand was present, the displacements were prevented from reaching the ground surface by local compaction of the loose sand layer. The soil displacement vectors immediately above the under-ream were observed to be approximately vertical and not at an angle to the under-ream. At peak capacity, smooth, 45° under-reamed piles therefore behaviour like plate anchors in two-layered sand, hence explaining the similar

F i o n a

Hughes
peak uplift capacities obtained for the plate anchor and two under-reamed piles tested in the pullout tests.

Post-peak, all the strains were mobilised in the loose upper layer and the displacements reached the ground surface for all layering configurations tested. The mean inclination of the soil displacement vectors immediately above the under-ream across all three tests was approximately 14° to the vertical, which is approximately equal to the interface friction angle between the aluminium under-ream and Hostun HN31 sand.

The implications of this research on the practical design of under-reamed piles are that if a pile embedded in a dense sand layer will only be subject to small strains, its performance will not be affected by the presence of a loose upper layer, provided there is a sufficient layer of dense sand above the under-ream. However, if the design relies upon the peak capacity or post-peak capacity, the performance of the pile will be significantly affected.

The lower bound solution proposed in this report assumes that the principal stress direction was rotated by an angle equal to that of the interface friction angle. As expected, this solution underestimates the experimental post-peak uplift capacity of the under-reamed piles for all layering configurations tested. With the exception of homogeneous loose sand, the upper bound solution proposed by Kumar (2003) also underestimates the experimental post-peak uplift capacity of the under-reamed piles tested. This unexpected observation is believed to be due to the incorrect assumption that normality is obeyed. This assumption imposes an uplift mechanism which involves a far greater volume of sand than has be observed in the half space tests and requires that there is no frictional resistance along the failure surface since there is no internal energy dissipation. An additional discrepancy between the failure mechanism observed in the present project and that obtained by Kumar (2003) is that the two layers were not observed to move as rigid blocks with the same velocity. In the tests conducted in this project, the ignored resistance due to friction along the failure surfaces appears to be greater than the resistance provided by the volume of sand which is incorrectly assumed to be within the failure mechanism. The difference between the magnitudes of these

F i o n a

Hughes
two inaccuracies appears to increase as the ratio of lower dense layer thickness to total embedment depth increases.

It must be noted that small scale model tests conducted at 1-g have much smaller soil confining stress levels than are usually experienced in the field. Therefore, it would be advised to conduct centrifuge model testing to confirm whether these conclusions are applicable to full sized under-reamed piles in the field.

8. Future Work

8.1 Small scale model testing

Small scale model testing is valuable as it enables a large number of comparative studies to be conducted with relative ease. To further investigate the uplift response of under-reamed pile foundations, recommendations for future small scale model testing include:

- additional half space tests using a range of under-ream angles, to observe the effect varying the under-ream angle has upon the failure mechanism geometry in two-layered sand.
- two-layered sand tests for a range of total embedment depths to investigate the relationship between layering configuration, total embedment, and uplift capacity.
- a comparative study between rough and smooth under-reamed pile foundations, to determine if changes in under-ream surface roughness have an effect on the uplift capacity and failure mechanism geometry.
- tests using a wider range of soil types. A wide range of soils are encounted in the field, including both dry and partially, or fully, saturated sand and clay. This project has focused wholly on dry sand; therefore tests on a wider range of soil types would be advisable. For saturated soils, the loading rate must be carefully controlled to govern whether the drained or undrained response is being measured. If the undrained response is being measured, pore pressure transducers should be used to measure the impact of pore pressure on the uplift response of the under-reamed pile.
- tests involving combined loading. The tests conducted in this project have only considered purely vertical loading on the under-reamed piles. However, in the field foundations are usually subject to combined loading, consisting of moments,

F i o n a

Hughes

horizontal shear and a vertical uplift or compressive force. Tests replicating these conditions would be advisable.

8.2 Large scale/centrifuge model testing

Small scale model tests conducted at 1-g have much smaller soil confining stress levels than are usually experienced in the field. As a consequence, far larger dilation angles are expected in small scale tests than in the field, causing a disparity between the responses of piles in the two cases (Dickin, 1988). The most beneficial plan for future work would involve centrifuge testing to allow the response of under-reamed pile foundations to be investigated at stresses comparable to those experienced in the field. It would be possible to use these tests to predict the load response of fully sized piles. Unfortunately, due to the time constraints associated with centrifuge testing, the number of tests conducted would be far less than is possible with small scale 1-g model testing.

It would be recommended to use centrifuge model testing to test the conclusions found in this report, as well as the recommendations for future work given in section 8.1.

8.3 Numerical studies

Numerical studies to investigate the performance of under-reamed pile foundations in non-cohesive soil would be advisable, since very little research has been conducted in this area. It would be valuable to understand whether the performance of under-reamed pile foundations could be successfully replicated numerically as, if this were possible, a large number of simulations of different conditions could be run with relative ease.

F i o n a

Hughes

References

Acar, Y. B., Durgunoglu, H. T. & Tumay, M. T., 1982. “Interface Properties of Sand”, *Journal of Geotechnical and Geoenvironmental Engineering*, Vol. 108 No. 4, pp. 648-654.

Balla, A., 1961. “The Resistance of Breaking out of Mushroom Foundations for Pylons”, *Proceedings of the 5th International Conference on Soil Mechanics and Foundation Engineering*. Paris, France, 17-22 July 1961. Paris: Dunod, pp. 569-576.

Bolton, M., 1979. *A Guide to Soil Mechanics*. London and Basingstoke: The Macmillan Press LTD.

Bouazza, A. & Finlay, T. W., 1990. “Uplift Capacity of Plate Anchors Buried in a Two-Layered Sand”, *Géotechnique*, Vol. 40 No. 2, pp. 293-297.

Bureau of Indian Standards, 1980. *IS:2911-3: Code of Practice for Design and Construction of Pile Foundations: Under-Reamed Piles*. New Delhi: Bureau of Indian Standards.

Cheuk, C. Y., White, D. J. & Bolton, M. D, 2008. “Uplift Mechanisms of Pipes Buried in Sand”, *Journal of Geotechnical and Geoenvironmental Engineering*, Vol. 134 No. 2, pp. 154-163.

Dickin, E. A., 1988. “Uplift Behaviour of Horizontal Plate Anchors in Sand”, *Journal of Geotechnical Engineering*, Vol. 144 No. 11, pp. 1300-1317.

Dickin, E. A. & Leung, C. F., 1990. “Performance of Piles with Enlarged Bases Subject to Uplift Forces”, *Canadian Geotechnical Journal*, Vol. 27 No. 5, pp. 546-556.

Dickin, E. A. & Leung, C. F., 1992. “The influence of foundation geometry on the uplift behaviour of piles with enlarged bases”, *Canadian Geotechnical Journal*, Vol. 29 No. 3, pp. 498-505.

Harris, D., 2014. “Uplift Resistance of an Under-Reamed Piled Foundation”, PR. Cambridge University Engineering Department: Fourth Year Undergraduate Project Report.

Harris, D. E. & Madabhushi, S. P. G., 2015. “Uplift Capacity of an Under-Reamed Pile Foundation”, *accepted by Proceedings of the ICE - Geotechnical Engineering*, Thomas Telford, London.

Hopkins, A., 2013. “The Uplift Capacity of Under-Reamed Piles”, PR. Cambridge University Engineering Department: Fourth Year Undergraduate Project Report.

F i o n a
Hughes
Ilamparuthi, K., Dickin, E. A. & Muthukrisnaiah, K., 2002. "Experimental Investigation on the Uplift Behaviour of Circular Plate Anchors Embedded in Sand", *Canadian Geotechnical Journal*, Vol. 39 No. 3, pp. 648-664.

Kumar, J., 2003. "Uplift Resistance of Strip and Circular Anchors in a Two Layered Sand", *Soils and Foundations*, Vol. 43 No. 1, pp. 101-107.

MATLAB R2014a, The MathsWorks, Inc., Natick, Massachusetts, United States.

Merifield, R. S. & Sloan, S, W., 2006. "The Ultimate Pullout Capacity of Anchors in Frictional Soils", *Canadian Geotechnical Journal*, Vol. 43 No. 8, pp. 852-868.

Meyerhof, G. G. & Adams, J. I., 1968. "The Ultimate Uplift Capacity of Foundations", *Canadian Geotechnical Journal*, Vol. 5 No. 4, pp. 225-244.

Mitrani, H., 2006. *Liquefaction Remediation Techniques for Existing Buildings*, Cambridge University: PhD Thesis.

Murray, E. J. & Geddes, J. D., 1987. "Uplift of Anchor Plates in Sand", *Journal of Geotechnical Engineering*, Vol. 113 No. 3, pp. 202-215.

Nagelschmidt, G., Desai, A. D. & Muir, A., 1940. "The Minerals in the Clay Fractions of a Black Cotton Soil and a Red Earth from Hyderabad, Deccan State, India", *The Journal of Agricultural Science*, Vol. 30 No. 4, pp. 639-653.

Potyondy, J. G., 1961. "Skin Friction Between Various Soils and Construction Materials", *Géotechnique*, Vol. 11 No. 4, pp. 339-353.

Rowe, R. K. & Davis, E. H., 1982. "The Behaviour of Anchor Plates in Sand", *Géotechnique*, Vol. 32 No. 1, pp. 25-41.

Sakai, T. & Tanaka, T., 2007. "Experimental and Numerical Study of Uplift Behaviour of Shallow Circular Anchor in Two-Layered Sand", *Journal of Geotechnical and Geoenvironmental Engineering*, Vol. 133 No. 4, pp. 469-477.

Subba Rao, K. S., Allam, M. M. & Robinson, R. G., 1996. "A Note on the Choice of Interfacial Friction Angle", *Proceedings of the ICE - Geotechnical Engineering*, Vol. 119 No. 1, pp. 1-6.

Subba Rao, K. S., Allam, M. M. & Robinson, R. G., 1998. "Interfacial Friction Between Sands and Solid Surfaces", *Proceedings of the ICE - Geotechnical Engineering*, Vol. 131 No. 2, pp. 75-82.

F i o n a
Hughes
Tomlinson, M. J., 2001. *Pile Design and Construction Practice*, 4th ed. London: Spon Press.

Uesugi, M. & Kishida, H., 1986. "Influential Factors of Friction Between Steel and Dry Sands", *Soils and Foundations*, Vol. 26 No. 2, pp. 33-46.

White D. J., Take, W. A. & Bolton, M. D., 2003. "Soil Deformation Measurement Using Particle Image Velocimetry (PIV) and Photogrammetry", *Géotechnique*, Vol. 53 No. 7, pp. 619-631.

White, D. J., Cheuk, C. Y. & Bolton, M. D., 2008. "The Uplift Resistance of Pipes and Plate Anchors Buried in Sand", *Géotechnique*, Vol. 58 No. 10, pp. 771-779.

Yoshimi, Y. & Kishida, T., 1981a. "A Ring Torsion Apparatus for Evaluating Friction Between Soil and Metal Surfaces", *Geotechnical Testing Journal*, Vol. 4 No. 4, pp. 145-152.

Yoshimi, Y. & Kishida, T., 1981b. "Friction Between Sand and Metal Surface", *Proceedings of the 10th International Conference on Soil Mechanics and Foundation Engineering*. Stockholm, Sweden, 15-19 June 1981. Rotterdam: Balkema, pp. 831-834.

Appendix: Risk Assessment Retrospective

A full risk assessment was undertaken prior to commencing experimental work. A mandatory induction to the laboratory at the Schofield Centre was also undertaken. The following hazards were identified and control measures were implemented:

Table 4: Hazards and control measures

Hazard	Control Measure(s)
Moving parts of the 1-D actuator	Remotely control it during experiments. Only physically handle it when the power supply is turned off.
Electrical equipment	Handle with due care.
Dust generated when pouring sand	Always wear a respirator mask when pouring sand. Seal off the room where pouring is taking place and use dust extractors.
Transportation of heavy items including sand bags, testing equipment and tests containers	Employ correct lifting procedures. Anything of sufficient weight to be seen as unsafe to carry alone must be lifted with the help of another, using a pallet truck or using a forklift truck (operated by a trained individual).
Computer use	A good seat with support must be used and breaks must be taken during lengthy periods of computer analysis and report writing.

The risk assessment conducted accurately reflected the hazards encountered during this project. No injuries were sustained during the project.

Due to the accuracy of the risk assessment conducted, if the project were to be repeated it would be recommended to access risk in the same way.